International Journal of
Molecular Sciences

MDPI

Article

Label-Free Investigations on the G Protein Dependent Signaling Pathways of Histamine Receptors

Ulla Seibel-Ehlert [1,*], Nicole Plank [1], Asuka Inoue [2], Guenther Bernhardt [1] and Andrea Strasser [1,*]

[1] Institute of Pharmacy, Faculty of Chemistry and Pharmacy, University of Regensburg, 93040 Regensburg, Germany; nicole.plank@ur.de (N.P.); guenther.bernhardt@ur.de (G.B.)
[2] Department of Pharmacological Sciences, Tohoku University, Sendai 980-8578, Japan; iaska@tohoku.ac.jp
* Correspondence: ulla.seibel@ur.de (U.S.-E.); andrea.strasser@ur.de (A.S.); Tel.: +49-941-943-2960 (U.S.-E.); +49-941-943-4821 (A.S.)

Abstract: G protein activation represents an early key event in the complex GPCR signal transduction process and is usually studied by label-dependent methods targeting specific molecular events. However, the constrained environment of such "invasive" techniques could interfere with biological processes. Although histamine receptors (HRs) represent (evolving) drug targets, their signal transduction is not fully understood. To address this issue, we established a non-invasive dynamic mass redistribution (DMR) assay for the human $H_{1–4}$Rs expressed in HEK cells, showing excellent signal-to-background ratios above 100 for histamine (HIS) and higher than 24 for inverse agonists with pEC_{50} values consistent with literature. Taking advantage of the integrative nature of the DMR assay, the involvement of endogenous $G\alpha_{q/11}$, $G\alpha_s$, $G\alpha_{12/13}$ and $G\beta\gamma$ proteins was explored, pursuing a two-pronged approach, namely that of classical pharmacology (G protein modulators) and that of molecular biology (Gα knock-out HEK cells). We showed that signal transduction of $hH_{1–4}$Rs occurred mainly, but not exclusively, via their canonical Gα proteins. For example, in addition to $G\alpha_{i/o}$, the $G\alpha_{q/11}$ protein was proven to contribute to the DMR response of $hH_{3,4}$Rs. Moreover, the $G\alpha_{12/13}$ was identified to be involved in the hH_2R mediated signaling pathway. These results are considered as a basis for future investigations on the (patho)physiological role and the pharmacological potential of $H_{1–4}$Rs.

Keywords: label-free; dynamic mass redistribution (DMR); G protein coupled receptors (GPCRs); histamine receptors; signaling pathways; G protein inhibitors; G protein knock-out

Citation: Seibel-Ehlert, U.; Plank, N.; Inoue, A.; Bernhardt, G.; Strasser, A. Label-Free Investigations on the G Protein Dependent Signaling Pathways of Histamine Receptors. *Int. J. Mol. Sci.* **2021**, *22*, 9739. https://doi.org/10.3390/ijms22189739

Academic Editor: Paul Chazot

Received: 12 August 2021
Accepted: 6 September 2021
Published: 9 September 2021

1. Introduction

G protein-coupled receptors (GPCRs), also termed seven-transmembrane-domain receptors (7TMs), are integral membrane proteins that transduce a broad variety of extracellular stimuli, ranging from photons and various small molecules to polypeptides, into the cell. As the largest superfamily of proteins in the human genome, GPCRs are involved in many (patho)physiological processes and represent important drug targets in the treatment of numerous diseases [1,2]. Canonical GPCR signal transduction occurs by binding of an agonist to a receptor, stabilizing an active receptor conformation and allowing the receptor to activate heterotrimeric G proteins, composed of Gα, Gβ and Gγ subunits. Upon GPCR activation, the G proteins dissociate from the receptor and split up into Gα and Gβγ subunits. Subsequently, both can modulate specific downstream effectors. The Gα proteins are divided into four major classes ($G\alpha_{q/11}$, $G\alpha_s$, $G\alpha_{i/o}$ and $G\alpha_{12/13}$), based on sequence similarity and their functional properties [3] and are predominantly associated with certain events in the signaling cascade, such as increase in intracellular Ca^{2+} and IP_3 ($G\alpha_{q/11}$), in- or decrease in cAMP level ($G\alpha_s$, $G\alpha_{i/o}$, respectively) or activation of Rho GTPase ($G\alpha_{12/13}$) [3,4]. By contrast, the effects of the Gβγ subunit are more diffuse [5,6]. Historically, GPCR signaling was assumed to occur via activation of a single class of Gα proteins, and therefore the receptors were typically classified accordingly [7].

However, scientific progress has revealed a complex network of signaling events including pleiotropic G protein (in-)dependent signaling, constitutive activity, biased agonism, receptor (hetero-)oligomerization and cross talk (reviewed in [8–11]).

To study these processes, a wide range of microtiter assay techniques are available [12–14]. For example, events very proximal to ligand binding, such as ligand induced conformational rearrangement of GPCRs [15], and activation and recruitment of (chimeric) G proteins [16] or β-arrestins [17] can be monitored. More distal in the signaling cascade, protein–protein interactions can be analyzed [18] as well as changes in the levels of second messengers (e.g., IP_3, Ca^{2+} and cAMP [19–22]) and the expression of gene reporters [20,23]. Despite numerous advantages, these "invasive" label-dependent methods spotlight only individual events in the complex GPCR signaling cascade and can produce system bias [24]. Moreover, the modification and co-expression of tagged proteins could alter the results. Another issue is that analyses of individual processes in the signaling cascade (yielding different readouts) require different experimental conditions and is often carried out in models of different cellular backgrounds (tissue bias). This makes the comparison between such results difficult.

Label-free approaches represent powerful "non-invasive" alternatives, able to capture the whole cellular response triggered by GPCR activation, independent of the signaling pathways involved and without the need to constrain specific experimental conditions. Therefore, label-free approaches such as optical dynamic mass redistribution (DMR) are gaining increasing attention both in drug discovery and GPCR signal transduction studies [25–28]. In a DMR assay, the measurement is based on the change of the refractive index near the biosensor (Figure 1A). This change is caused by a reorganization of cellular components, accompanied by a morphological rearrangement of the cells. In GPCR research, this is triggered by stimulation of a receptor with a ligand [29,30]. As the change in refractive index is measured relative to a baseline, the DMR response can be positively or negatively deflected, depending on both the cell model and the receptor-ligand combination used. Therefore, the DMR signal is a holistic response, reflecting multiple cellular events downstream of receptor activation. Such dynamic response profiles are used to quantify various types of ligand action, including full, partial and inverse agonism, antagonism and allosteric modulation in both native [31,32] and recombinant [33] expression systems. However, due to the complexity of the DMR response, it is difficult to identify which events are reflected by the DMR signal, a phenomenon referred to as a "black box" [34]. Although certain characteristics of the signaling profiles of GPCRs in label-free responses were attributed to the activation of distinct classes of Gα proteins [26,29,35,36], there is also evidence to the contrary [37]. Application of G protein modulators such as pertussis toxin (PTX), FR900359 (FR) and cholera toxin (CTX) [37–39] can be used to dissect these G protein dependent signals [37]. PTX selectively and irreversibly inactivates the $G\alpha_{i/o}$ protein by ADP-ribosylation at the Gα-subunit [20,33,37,40–42]. CTX locks the $G\alpha_s$ protein in its GTP bound state by irreversible ADP-ribosylation, leading to a permanent activation of the $G\alpha_s$ protein, which is in turn uncoupled and no longer available for GPCR recruitment [31–33,37,43]. As ribosylation leads to a maximum activation of the $G\alpha_s$ protein rather than inhibition of the $G\alpha_s$ protein, the results should be interpreted with caution. FR (alias UBO-QIC) selectively silences $G\alpha_{q/11}$ signaling by blocking the GDP-release in the Gα subunit [18,41,44–47], which is a mandatory step in G protein activation. The advantage of such studies is that they can be performed with the same cell model under identical experimental conditions, thereby precluding cell bias. Such investigations have already been performed for a variety of GPCRs [37,38,47–53]. Another approach to investigate the involvement of G proteins in signal transduction is to prevent their expression by knocking out the corresponding genes [41,54,55]. An advantage of the knock-out strategy over the administration of G protein modulators is the chance that the G protein can be switched off more precisely. In this study, both approaches were followed to investigate the G protein signaling pathways of histamine $hH_{1–4}$ receptors by DMR.

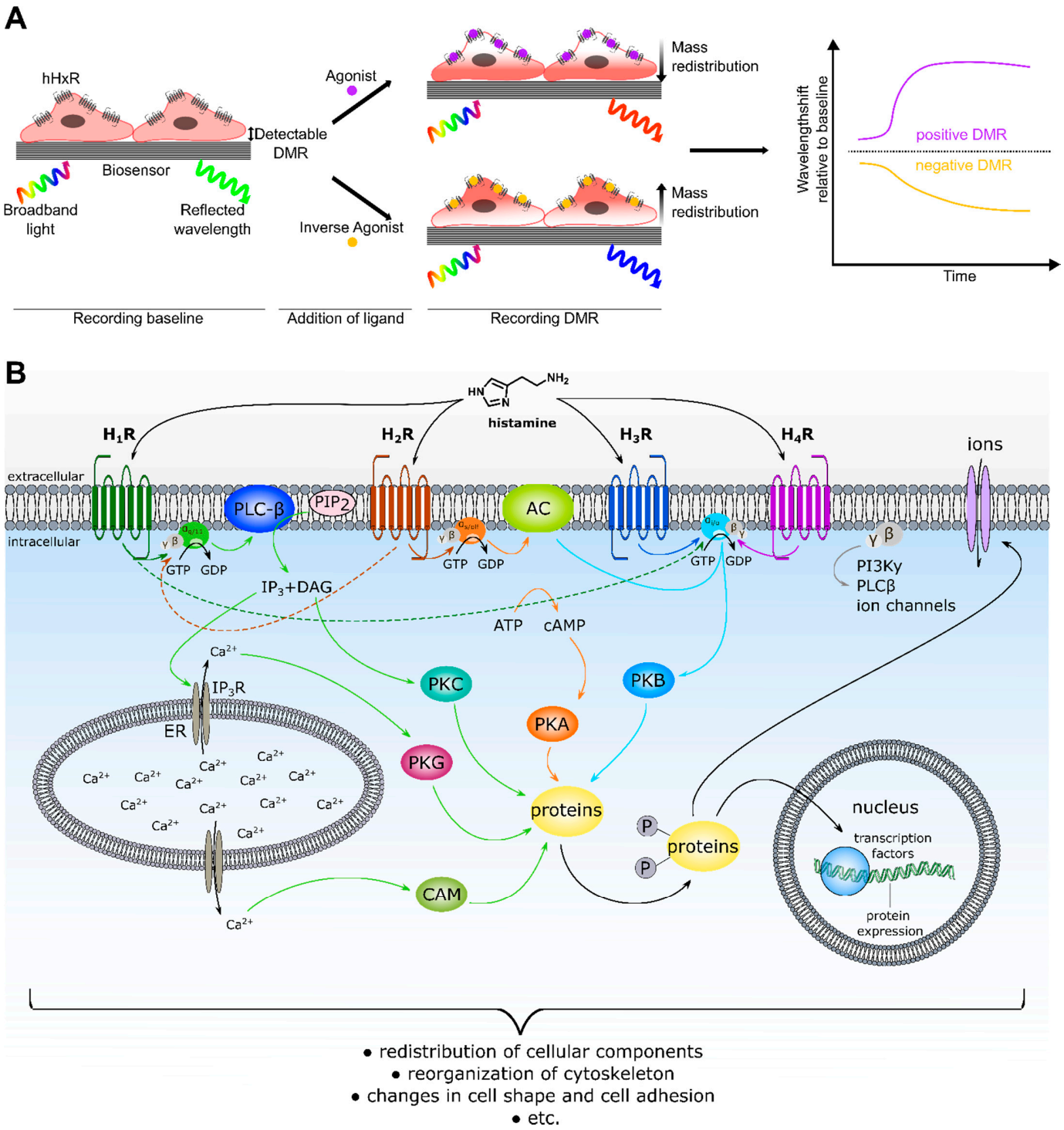

Figure 1. Schematic illustrations of the principle of the DMR assay and canonical signal transduction of histamine $H_{1–4}$Rs. (**A**) The label-free DMR technology detects changes in the refractive index caused by mass redistribution inside a cell, triggered by receptor stimulation, relative to a baseline. Alteration of the refractive index is measured with a biosensor, integrated in each well of a microplate (adapted from Schröder et al. [38]). (**B**) Schematic summary of the signal transduction of $H_{1–4}$Rs according to IUPHAR [56] and Panula et al. [57] (adapted from Panula et al. [57]). Canonical Gα protein signaling is indicated by solid lines. Involvement of secondary Gα proteins is indicated by dashed lines. AC, adenylyl cyclase; CAM, calcium-modulated protein; CTX, cholera toxin; DAG, diacylglycerol; IP_3, inositol-1,4,5-trisphosphate; PI3Kγ, phosphoinositide 3-kinase-γ; PIP_2, phosphatidylinositol-4,5-bisphosphate; PKA, protein kinase A; PKB, protein kinase B; PKC, protein kinase C; PLC-β, phospholipase C-β; PTX, pertussis toxin.

Histamine receptors (HRs) represent important drug targets in the treatment of disorders, such as allergy and reflux diseases [58]. They transmit their signals predominantly via three classes of G proteins: H_1 via $G\alpha_{q/11}$, H_2 via $G\alpha_s$ and H_3 + H_4 via $G\alpha_{i/o}$ (Figure 1B). However, for the H_1 and H_2 receptors, evidence is emerging for promiscuous activation of Gα proteins [59–61]. By contrast, less information is available on the involvement of non-canonical G protein subunits in the signal transduction processes of the $H_{3,4}$Rs. The first aim of the study was to establish a DMR assay for the entire histamine receptor family to compare the signaling patterns of the $H_{1–4}$Rs in the same experimental setup. For this purpose, the four human receptor subtypes ($hH_{1–4}$Rs) were stably expressed in HEK cells. HEK cells were chosen as they constitutively express the four relevant Gα classes ($G\alpha_s$, $G\alpha_{q/11}$, $G\alpha_{12/13}$ and $G\alpha_{i/o}$) at comparable levels [62]. The contribution of G proteins to the integrated DMR response of $hH_{1–4}$Rs was investigated by pursuing two different approaches. Firstly, in a classical pharmacological approach the G protein signaling pathways in HEK $hH_{1–4}$R cells were silenced using G protein modulators (PTX, CTX, FR and gallein). Secondly, in a molecular biological approach CRISPR/Cas 9 modified Gα knock-out HEK cells ($\Delta G\alpha_x$ HEK) lacking either the $G\alpha_{s/l}$ ($\Delta G\alpha_{s/l}$ HEK) [63], the $G\alpha_{q/11}$ ($\Delta G\alpha_{q/11}$ HEK) [44] or the $G\alpha_{12/13}$ ($\Delta G\alpha_{12/13}$ HEK) [64] gene were stably transfected with $hH_{1–4}$Rs. Moreover, cells lacking six Gα proteins ($\Delta G\alpha_{s/l,\ q/11,\ 12/13}$ = $\Delta G\alpha_{six}$ HEK) [41], stably expressing the $hH_{1–4}$Rs were used. The results for both approaches were compared and discussed with respect to the impact of G protein inactivation on the $hH_{1–4}$R mediated DMR response.

2. Results and Discussion

2.1. Characterization of HEK $hH_{1–4}$R Cells

To investigate the effect of endogenously expressed G proteins on the DMR response, HEK $hH_{1–4}$R cells were generated. For this purpose, the human histamine H_1, H_2, H_3 or H_4 receptor ($hH_{1–4}$Rs) was inserted into a pIRESneo3 vector encoding the signaling peptide (SP) of the murine 5-HT_{3A} receptor and a FLAG tag to give the pIRESneo3-SP-FLAG-$hH_{1–4}$R constructs. Both parental and $\Delta G\alpha_x$ HEK cells were stably transfected with these constructs to give HEK $hH_{1–4}$R and $\Delta G\alpha_x$ HEK $hH_{1–4}$R cells. For HEK $hH_{1–4}$R cells, single clones of the stable transfectants were picked, selected, and screened by DMR for the highest signal elicited by 100 µM histamine (data not shown; (structure is presented in supplementary Figure S1). The expression of the $hH_{1–4}$Rs in HEK cells was confirmed by radioligand saturation binding using live cells (Supplementary Figure S2). For the characterization of the $\Delta G\alpha_x$ HEK $hH_{1–4}$R cells see Section 2.4.1 and supplementary Figure S3. The expression levels of $hH_{1–4}$Rs in HEK $hH_{1–4}$R cells were calculated using B_{max} and the specific activity (a_s) of the corresponding radioligand and the cell number (Table 1). Despite identical receptor cloning and transfection procedures of the $hH_{1–4}$Rs, the expression level of hH_3R and hH_4R was lower compared to the hH_1R and hH_2R. The pK_d values determined for the respective radioligands at HEK $hH_{1–4}$R cells were in good agreement with literature data (Table 1).

To further characterize the HEK $hH_{1–4}$R cells, radioligand competition binding experiments were performed with histamine (HIS) and one receptor-specific, inverse agonist (diphenhydramine (DPH) at the hH_1R, famotidine (FAM) at the hH_2R, pitolisant (PIT) at the hH_3R and thioperamide (THIO) at the hH_4R) using live cells (structures are presented in supplementary Figure S1). The displacement curves are shown in supplementary Figure S4 and the pK_i values are summarized in Table 2. As expected, HIS had a markedly higher affinity to $hH_{3,4}$Rs compared to $hH_{1,2}$Rs (Table 2). In the literature, pK_i values were determined either with cell membranes/homogenates or with live cells. In general, the pK_i values determined for HIS and the inverse agonists using HEK $hH_{2–4}$R cells were in the same range as reported in the literature with live cells (Supplementary Table S1). To the best of our knowledge, pK_i values for HIS at the hH_1R in live cells have not yet been reported. Compared to reference values from membranes/homogenates ranging between 4.3–5.9 [65–67], the affinity of HIS for the hH_1R was lower in live cells (pK_i = 3.37 ± 0.29).

The use of live cells in comparison to membrane preparations has a marked influence of the "apparent affinity" of ligands, especially in the case of agonists [68].

Table 1. Radioligand saturation binding data determined with live HEK $hH_{1-4}R$ and $\Delta G\alpha_x$ HEK $hH_{1-4}R$ cells using [^{3}H]MEP, [^{3}H]UR-DE257 or [^{3}H]UR-PI294 as radiolabeled tracers for hH_1R, hH_2R or $hH_{3,4}R$, respectively.

G Protein Knock-Out (Δ)	HR	Binding Sites/Cell	pK_d	*n*	pK_d Ref.
none	hH_1R	$2.50 \times 10^6 + 0.52 \times 10^6$	8.32 + 0.08	4	8.36 [a]
$\Delta G\alpha_{s/l}$	hH_1R	$6.16 \times 10^5 + 2.07 \times 10^5$	8.42 + 0.04	3	
$\Delta G\alpha_{q/11}$	hH_1R	$1.78 \times 10^5 + 0.26 \times 10^5$	8.61 + 0.18	3	
$\Delta G\alpha_{12/13}$	hH_1R	$2.18 \times 10^5 + 0.04 \times 10^5$	8.46 + 0.08	3	
$\Delta G\alpha_{six}$	hH_1R	Not detectable		3	
none	hH_2R	$2.43 \times 10^6 + 0.23 \times 10^6$	7.19 + 0.06	6	7.26 [b]
$\Delta G\alpha_{s/l}$	hH_2R	$1.68 \times 10^6 + 0.33 \times 10^6$	7.37 + 0.19	3	
$\Delta G\alpha_{q/11}$	hH_2R	$9.37 \times 10^6 + 0.63 \times 10^6$	7.40 + 0.06	3	
$\Delta G\alpha_{12/13}$	hH_2R	$3.94 \times 10^6 + 0.12 \times 10^6$	7.98 + 0.05 ****	3	
$\Delta G\alpha_{six}$	hH_2R	$4.23 \times 10^6 + 0.03 \times 10^6$	7.86 + 0.06 ***	3	
none	hH_3R	$1.01 \times 10^5 + 0.21 \times 10^5$	8.61 + 0.03	3	8.96 [c]
$\Delta G\alpha_{s/l}$	hH_3R	$3.20 \times 10^4 + 0.83 \times 10^4$	8.71 + 0.11	3	
$\Delta G\alpha_{q/11}$	hH_3R	$3.94 \times 10^4 + 0.93 \times 10^4$	8.73 + 0.02	2	
$\Delta G\alpha_{12/13}$	hH_3R	$4.63 \times 10^4 + 1.32 \times 10^4$	8.49 + 0.10	3	
$\Delta G\alpha_{six}$	hH_3R	$1.01 \times 10^5 + 0.32 \times 10^5$	8.41 + 0.18	3	
none	hH_4R	$1.37 \times 10^5 + 0.18 \times 10^5$	8.45 + 0.05	4	8.26 [d]
$\Delta G\alpha_{s/l}$	hH_4R	$1.42 \times 10^5 + 0.33 \times 10^5$	8.26 + 0.07	4	
$\Delta G\alpha_{q/11}$	hH_4R	$1.24 \times 10^5 + 0.11 \times 10^5$	8.54 + 0.02	3	
$\Delta G\alpha_{12/13}$	hH_4R	$5.23 \times 10^4 + 0.42 \times 10^4$	8.55 + 0.06	3	
$\Delta G\alpha_{six}$	hH_4R	$1.06 \times 10^5 + 0.20 \times 10^5$	8.22 + 0.08	4	

Data is presented as means ± SEM of at least three independent experiments, each performed in triplicate. Reference data was transformed from K_d to pK_d values. [a] Saturation binding experiments with live HEK-CRE-Luc hH_1R hMSR1 cells and [^{3}H]MEP [20]. [b] Saturation binding experiments with live HEK-CRE-Luc hH_2R cells and [^{3}H]UR-DE257 [69]. [c] Saturation binding experiments with membrane preparations of Sf9 insect cells co-expressing the hH_3R + $G\alpha_i$ + $G\beta\gamma$ and [^{3}H]UR-PI294 [70]. [d] Saturation binding experiments with membrane preparations of Sf9 insect cells co-expressing the hH_4R + $G\alpha_i$ + $G\beta\gamma$ and [^{3}H]UR-PI294 [70]. Statistical difference in pK_d value among HR subtypes relative to the control (e.g., HEK hH_1R (control) versus $\Delta G\alpha_x$ HEK hH_1R) was analyzed by one-way ANOVA followed by Dunnett's multiple comparison test calculated as *** $p \leq 0.001$, **** $p \leq 0.0001$.

2.2. Establishment of a DMR Assay Using HEK $hH_{1-4}R$ Cells

2.2.1. Stimulation of HEK $hH_{1-4}R$ Cells with Histamine

HEK $hH_{1-4}R$ cells were stimulated with increasing HIS concentrations and the DMR response was recorded for 60 min. Positively deflected and concentration dependent DMR traces were observed for all four HR subtypes (Figure 2A), where both the signal maximum and the time course varied depending on the HR subtype. Of note, no DMR response was detected in non-transfected HEK wildtype (wt) cells, neither for HIS nor for inverse agonists (Supplementary Figure S6A), demonstrating that the ligand induced DMR responses observed in HEK $hH_{1-4}R$ cells were HR mediated.

The highest amplitude and fastest increase in the DMR response was observed in HEK hH_1R cells (1000 pm after 15 min; 10 µM HIS).

This kinetic profile of HIS induced DMR in HEK hH_1R cells shows similarity to that observed in HeLa cells, which express the hH_1R endogenously [71]. In HeLa cells, the positive DMR showed a peak response of approx. 300 pm within 3–5 min upon HIS addition, which decreased slightly and remained stable thereafter [71]. In A431 cells, which also express the hH_1R endogenously, the positive DMR signal increased to a maximum value of approx. 500 pm within approx. 5 min after addition of HIS [72]. Afterwards, the DMR signal decreased steadily to the level of the baseline [72]. A similar kinetic profile was observed previously in our group using genetically engineered HEK293T-CRE-Luc-H_1R-hMSR1 cells where the hH_1R was co-expressed with the human macrophage scavenger receptor 1 (hMSR1), introduced to enhance the adhesion of HEK cells [20]. In

HEK293T-CRE-Luc-H_1R-hMSR1 cells, the positive DMR peaked at approx. 600 pm within 10 min after HIS addition and gradually decreased afterwards back to baseline [20,73]. These disparate kinetic profiles observed after stimulation of the hH_1R with HIS were not surprising, as many characteristics of the different cell models used, e.g., receptor expression, expression patterns of (G) proteins, and/or cell adhesion, can affect the kinetic profile of the DMR response [73,74]. When comparing the kinetics of HIS in HEK hH_1R cells with DMR traces of purinergic P2Y or muscarinic M3 receptors (both also $G\alpha_q$ coupled and heterologously expressed in HEK cells) [44], no similarities were found.

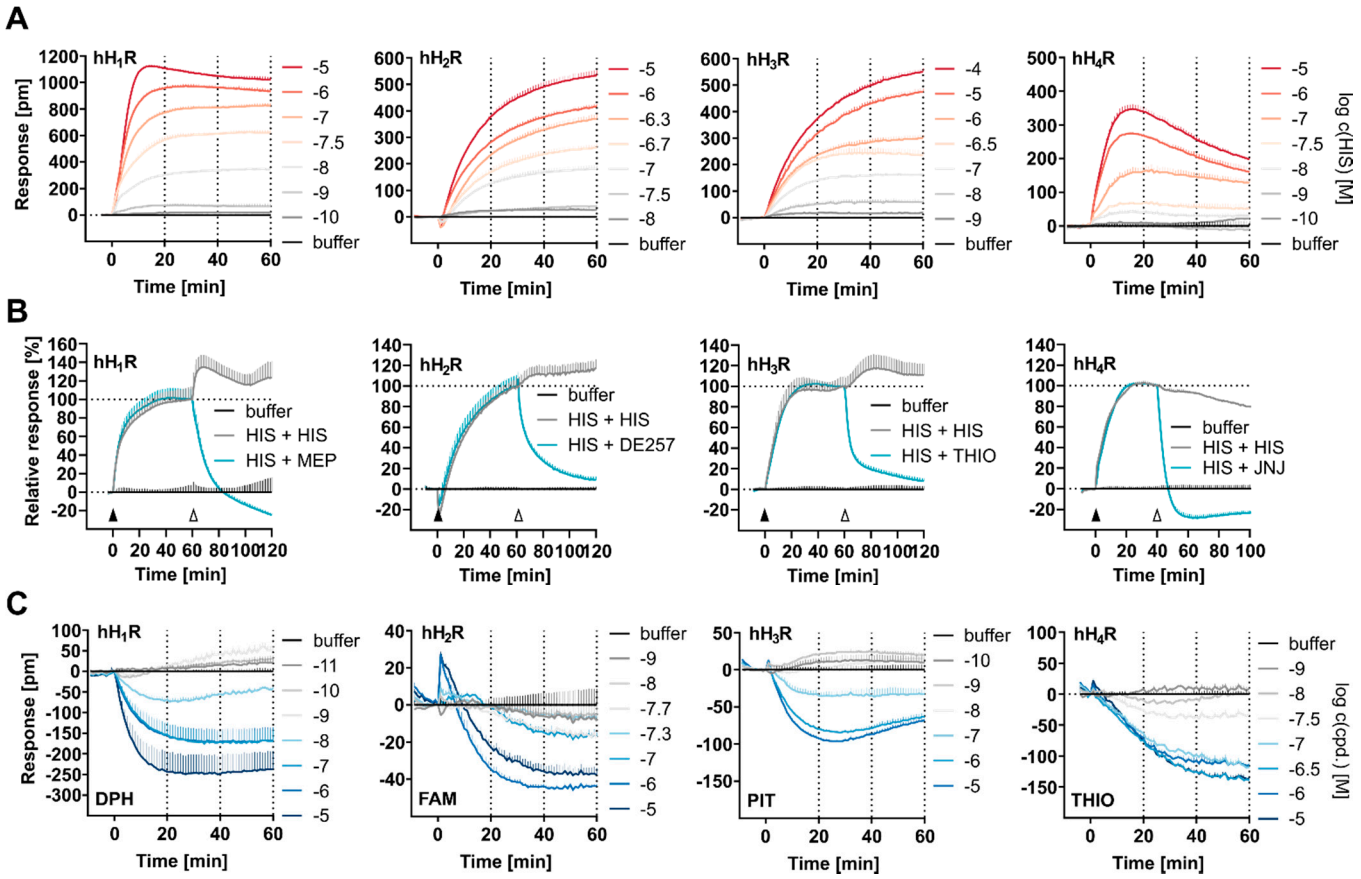

Figure 2. Implementation of the DMR assay for the $hH_{1-4}Rs$ stably expressed in HEK cells. (**A**) Representative DMR traces recorded with HEK $hH_{1-4}R$ cells upon stimulation with increasing concentrations of histamine. (**B**) The histamine induced DMR responses were reversible in HEK $hH_{1-4}R$ cells. The HEK $hH_{1-4}R$ cells were pre incubated with histamine at concentrations corresponding to the respective pEC_{80} value (hH_1R = 316 nM, hH_2R = 794 nM, hH_3R = 1995 nM, hH_4R = 501 nM, indicated by the filled arrow ▲) and the DMR response was recorded for 60 min ($hH_{1-3}R$) or for 40 min (hH_4R). Subsequently, a receptor specific antagonist was added (hH_1R 10 µM MEP, hH_2R 10 µM DE257, hH_3R 10 µM THIO, hH_4R 10 µM JNJ, empty arrow △) and the DMR was recorded for additional 60 min. (**C**) Constitutive activity was detected in HEK $hH_{1-4}R$ cells. Inverse agonism was observed at the hH_1R for DPH, at the hH_2R for FAM, at the hH_3R for PIT, at the hH_4R for THIO. Traces shown in (**A**–**C**) were corrected for the buffer and represent mean ± SEM of the technical triplicate. Traces shown in (**B**) were additionally normalized to the value recorded after 60 min (100%).

Compared to HEK hH_1R cells, the DMR response recorded for HEK hH_2R and HEK hH_3R cells were markedly different, showing no sharp maxima upon stimulation with HIS at a concentration of 10 or 100 µM within 60 min. Instead, the DMR signal increased slower, but steadily, reaching a highest amplitude ranging between 500–600 pm after 60 min. A unique feature of the hH_2R mediated DMR response was a slight signal dip (Zoom-in in supplementary Figure S5) immediately after HIS addition, a phenomenon that was not observed within this study for any other HR subtype under the same experimental conditions. A signal dip was also observed for the $G\alpha_s$ coupled GPCRs [29,37], e.g., EP2/4,

which was stably expressed in HEK cells [37]. Ye Fang [29] explained such a signal dip by the fact that downstream signaling components involved in the signal transduction process are already compartmentalized and located at or near the cell membrane. Therefore, the recruitment of intracellular signal transduction components to activated receptors is less pronounced and other cellular signaling events are more salient leading to an initial decrease in local mass density [29]. However, one should be careful to interpret this as a reliable feature of $G\alpha_s$ coupling.

Although the hH_2R is reported as $G\alpha_s$ coupled [57] and the hH_3R is described as a $G\alpha_{i/o}$ coupled receptor [57], the DMR traces recorded upon stimulation with HIS were similar in both signal amplitude and time course, except for the signal dip in the case of the hH_2R (Figure 2A). This was surprising as we had expected that different G protein coupling would be associated with distinct DMR signaling profiles. Moreover, it was interesting that the signal amplitudes were similar because the expression level of the hH_3R was approximately 20-fold lower compared to that of hH_2R (Table 1), conflicting with the assumption that the signal amplitude is positively correlated with the level of receptor expression. Instead, it can be speculated that the receptor-specific signal transduction pathway plays a role.

Even though both the $hH_{3,4}Rs$ are structurally related and considered as $G\alpha_{i/o}$ coupled receptors (Figure 1B), the recorded DMR traces of HEK hH_3R and hH_4R cells differed in both time course and signal amplitude (Figure 2A). Among the four human HR subtypes analyzed in this study, the lowest DMR response was recorded in HEK hH_4R cells. The signal reached its maximum of approx. 300–400 pm within 10–20 min at the highest HIS concentration of 10 µM, and then declined continuously. Various $G\alpha_{i/o}$ coupled receptors expressed in HEK cells (DP2 [41], CRTH2 [44]) or in CHO cells (NOP [75]) showed comparable kinetic profiles in DMR assays.

2.2.2. Reversibility of HIS Induced DMR

To demonstrate the reversibility of the DMR responses, HEK $hH_{1–4}R$ cells were first treated with histamine at concentrations corresponding to the respective pEC_{80} value (hH_1R = 316 nM, hH_2R = 794 nM, hH_3R = 1995 nM, hH_4R = 501 nM; indicated by the filled arrow in Figure 2B) and the DMR was recorded for 60 min with HEK $hH_{1,2,3}R$ cells, or for 40 min with HEK hH_4R cells. In the second step, a receptor-specific antagonist was added (10 µM mepyramine (MEP) for hH_1R, 10 µM DE257 for hH_2R, 100 µM thioperamide (THIO) for hH_3R and 10 µM JNJ7777120 (JNJ) for hH_4R; indicated by the empty arrow in Figure 2B; structures of antagonists are presented in supplementary Figure S1). As a control, HEK $hH_{1–4}R$ cells were also stimulated with HIS, but in the second step, instead of an antagonist, HIS was added at a concentration corresponding to the pEC_{80}. This was to ensure that the observed effect was induced by the antagonist and not by the addition procedure disturbing the system. For all four HR subtypes, the HIS-induced signal was suppressed by addition of a receptor subtype-specific antagonist, and no decrease in the signal was observed in the controls, showing reversibility of the DMR signal.

2.2.3. Constitutive Activity

Previously, all four HR subtypes have been reported as constitutively active in heterologous expression systems in canonical assays [23,76–81]. Constitutive (basal) activity describes the ability of GPCRs to produce a biological response in the absence of agonist binding by spontaneously adopting an active conformation [82]. Usually, the measurement of constitutive activity occurs by comparing the basal activity of a system comprising active-state receptors (e.g., transfected cells or high receptor expression) and without receptors (e.g., not transfected cell, low receptor expression) [83]. The basal activity should increase with increase in receptor expression. To assess the constitutive activity of HRs in the DMR assay we compared the DMR traces of the buffer controls (assay buffer w/o ligand) recorded for not transfected HEK cells with that recorded for HEK $hH_{1–4}R$ cells (Supplementary Figure S7). After an equilibration period of about 40 min, higher basal

activity was measured in HEK $hH_{1,3,4}Rs$ compared to not transfected HEK wt cells. We interpret this as an indication that the receptors in this system are constitutively active. However, no difference in the basal activity was observed between HEK hH_2R cells and HEK wt cells (Supplementary Figure S7). This may imply that the hH_2R is either not constitutively active in this system, or that this activity is too weak to be detected in this system. To explore measurement of inverse agonism by DMR, HEK $hH_{1-4}R$ cells were stimulated with a receptor specific inverse agonist (hH_1R: DPH, hH_2R: FAM, hH_3R: PIT, hH_4R: THIO) at increasing concentrations. Constitutive activity, manifesting as negatively deflected DMR traces, was observed at all four receptor subtypes, differing in intensity depending on the HR-ligand combination. (Figure 2C). The weakest inverse activity was measured for the hH_2R when stimulated with FAM. This implies that the hH_2R is constitutively active, but much lower compared to $hH_{1,3,4}R$. We previously anticipated this to be the case in view of supplementary Figure S7. We can rule out off-target effects for any HR-ligand combination, as none of the ligands elicited a DMR response in not transfected HEK wt cells (Supplementary Figure S6A).

2.2.4. Assay Quality

For data analysis, the area under curve (AUC) was calculated for the DMR traces, which is a commonly applied concept for the assessment of dynamic pharmacological processes [38,73]. Compared to single point measurements, the integration over time provides a more accurate estimate of the overall response to a drug [84]. To assess assay quality, signal-to-background (S/B) ratios were estimated based on AUC over the entire measurement period of 60 min (AUC_{60}) for both HIS and a respective inverse agonist using HEK $hH_{1-4}R$ cells. We are aware that the calculation of the S/B ratio using AUC appears problematic as the DMR signal does not represent an absolute measure, but rather a shift of the wavelength relative to the baseline. To alleviate this problem, we considered the stable baseline as the zero point and used the modulus of AUC for the estimation of the S/B ratio. This approximation is possible because the EnSpire software records and uses the last measuring point (repeat) in the baseline run as the calibration offset, which is subtracted from all repeats of the baseline and the final record (last repeat in the baseline was set to zero) [85].

For HIS, high S/B ratios were determined at the hH_1R, hH_2R, hH_3R and hH_4R, amounting to 308, 277, 218 and 123, respectively (Figure 3). Compared to HIS, the S/B ratios for the standard inverse agonists were markedly lower (S/B ratios: DPH (hH_1R) = 53, FAM (hH_2R) = 33, PIT (hH_3R) = 25 and THIO (hH_4R) = 30) as shown in Figure 3. In comparison, S/B ratios for HIS in [^{35}S]GTPγS or miniG assays ranged from 2 to 30 [80]. Among other factors, high S/B ratios are beneficial for signal deconvolution studies, assessing efficacies and potencies of ligands, and investigating constitutive activities of receptors.

2.2.5. Conversion of the DMR Responses to Concentration-Response-Curves (CRCs)

The optical traces (representations in Figure 2A, C) were converted to CRCs by calculating the AUC_{60} and plotting these values against the logarithmic concentrations of a compound (Figure 4A). The determined pEC_{50} and E_{max} values are summarized in Table 2. However, when calculating the S/B ratios, a slight dependency on the time interval used for the AUC calculations was observed (described in SM Text S1, Impact of the time interval used for calculations of AUC on S/B ratios, supplementary Figure S8 and supplementary Table S3). Moreover, a time-dependent potency of agonists was observed at the muscarinic M_3 [86] and the neurotensin NTS_1 [53] receptor in DMR assays. Therefore, we investigated whether the time interval used to calculate the AUC had an impact on the pEC_{50} and E_{max} values of HIS and the receptor specific inverse agonists.

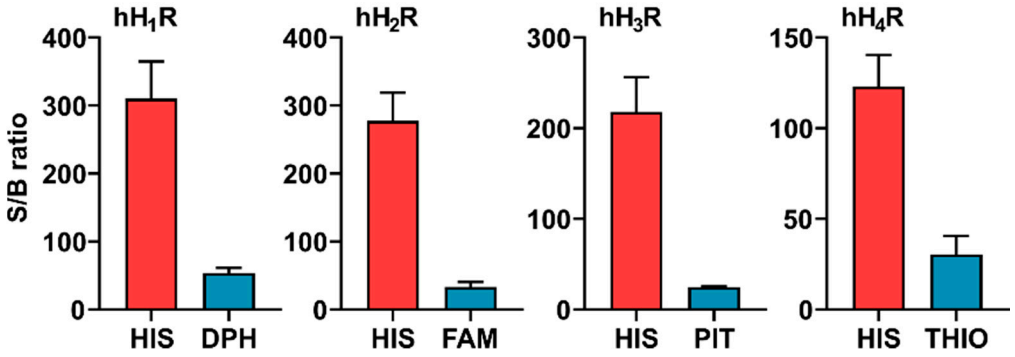

Figure 3. Signal-to-background (S/B) ratios estimated for HIS and inverse agonists using HEK $hH_{1–4}R$ cells. For the estimation of S/B values, the modulus of area under curve (AUC_{60}) was calculated for the highest concentrations of HIS (10 µM in HEK $hH_{1,2,4}R$ cells and 100 µM in HEK hH_3R cells) and the respective inverse agonist (10 µM DPH in HEK hH_1R cells, 10 µM FAM in HEK hH_2R cells, 10 µM PIT in HEK hH_3R cells, 100 µM THIO in HEK hH_4R cells), and divided by the respective AUC_{60} value determined for the buffer. For HIS, the positive AUC (above baseline) was used, whereas for the inverse agonists the negative AUC (below baseline) was calculated. The S/B ratios are presented as mean ± SEM from at least three independent experiments, each performed in triplicate.

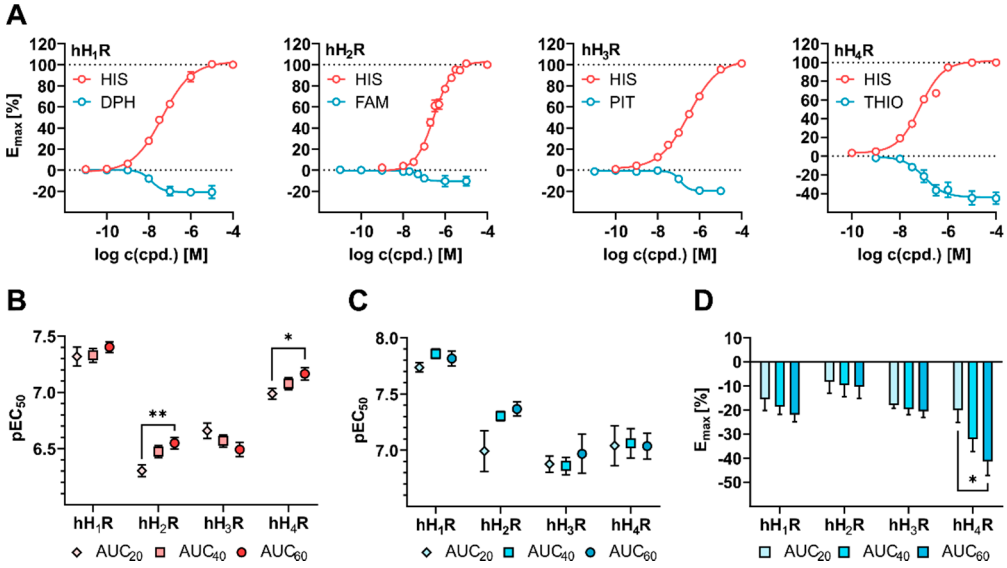

Figure 4. Analysis of DMR responses elicited by HIS (**red**) and inverse agonists (**blue**) in HEK $hH_{1–4}R$ cells. (**A**) CRCs determined for HIS and indicated inverse agonists at the $hH_{1–4}Rs$ using AUC_{60}. The E_{max} values determined for the inverse agonists wee normalized to the highest histamine concentration applied for the respective receptor subtype. (**B**) pEC_{50} values for HIS resulting from CRCs constructed by using AUC_{20}, AUC_{40} or AUC_{60} at the $hH_{1–4}Rs$. (**C**) pEC_{50} values calculated for inverse agonists (DPH at the hH_1R, FAM at the hH_2R, PIT at the hH_3R and THIO at the hH_4R) resulting from CRCs constructed by using AUC_{20}, AUC_{40} or AUC_{60} at the $hH_{1–4}Rs$. (**D**) E_{max} values determined for DPH at the hH_1R, FAM at the hH_2R, PIT at the hH_3R and THIO at the hH_4R using the AUC_{20}, AUC_{40} or AUC_{60}. E_{max} values were normalized to the highest HIS concentration applied for the corresponding HR subtype. (**A**–**D**) All values are means ± SEM of at least three independent experiments, each performed in triplicate. Statistical difference relative to AUC_{60} was analyzed by one-way ANOVA followed by Dunnett's multiple comparison test calculated as * $p \leq 0.05$, ** $p \leq 0.01$.

For this purpose, additional CRCs were constructed using AUC calculations after 20 or 40 min ($AUC_{20, 40}$) and compared to those from AUC_{60} (Supplementary Figure S9 and supplementary Table S4). For HEK hH_1R cells, the time interval had no impact on

the mean pEC_{50} values for HIS (Figure 4B). By contrast, in HEK hH_2R and hH_4R cells a significant increase in pEC_{50} values from AUC_{20} to AUC_{60} was observed for HIS (hH_2R: from 6.30 ± 0.05 to 6.57 ± 0.05; hH_4R: from 6.99 ± 0.05 to 7.15 ± 0.05, respectively), whereas in HEK hH_3R a gradual decrease in mean pEC_{50} values was observed from AUC_{20} to AUC_{60} (from 6.66 ± 0.07 to 6.49 ± 0.06), which, however, was statistically not significant. For inverse agonists, the calculation of AUC after 20, 40 and 60 min had no significant impact on the mean pEC_{50} values (Figure 4C). Signal transduction of GPCRs involves a complex network of different spatially and temporally resolved events, each of which show individual kinetics and/or amplitudes [53,86,87]. As all this information is bundled in the DMR response, it was not surprising that the temporal component could have an impact on the pEC_{50} and E_{max} value depending on the specific signaling cascade triggered by the receptor ligand interaction. The E_{max} values gradually decreased from AUC_{20} to AUC_{60} for all four HR-inverse agonist combinations (Figure 4D; exact values in supplementary Table S4) but particularly for THIO at hH_4R, where the mean E_{max} value showed a significant decrease from AUC_{20} to AUC_{60} ($E_{max}(AUC_{20}) = -20.1 \pm 5.0$ to $E_{max}(AUC_{60}) = -45.0 \pm 5.7$). The slow kinetics of the DMR response recorded for the inverse agonists can be considered as an explanation here (Figure 2A (HIS) versus Figure 2C (inverse agonists). In view of these results, the inclusion of the entire kinetic information (AUC_{60}) appears preferable and was considered as the standard method to calculate pEC_{50} and E_{max} values in the following experiments.

2.2.6. Functional Characterization of (Inverse) Agonists: Label-Free DMR versus Label-Dependent Techniques

There was a discrepancy between competition binding and DMR functional data determined for HIS using HEK $hH_{1,2}R$ cells (Table 2). The pK_i values for HIS in live cells were approximately 4 (hH_1R) or 2 (hH_2R) orders of magnitude lower compared to the pEC_{50} values in the DMR assay. Moreover, a discrepancy between affinity and potency was observed for pitolisant (PIT) at the hH_3R, where the pK_i value was about 2 orders of magnitude larger compared to the pEC_{50} value in the DMR assay. As binding data reflect the strength of the receptor-ligand interaction, whereas functional responses are amplified translations of the receptor-ligand interaction, differences in this range are not uncommon and have been reported for example, for dopamine receptors [88]. We have previously stimulated HEK293T-CRE-Luc-hH_1R-hMSR1 cells with HIS at increasing concentrations in the DMR assay [20]. The CRCs from AUC_{40} revealed a pEC_{50} value of 7.49 [20], which agrees with the result reported here (pEC_{50} = 7.38 ± 0.05).

Table 2. Summary of binding and functional data determined on live HEK $hH_{1-4}R$ cells and reference data.

		Determined			References			
		Comp Bdg	DMR		miniG Recruitment [80]		Luciferase Reporter Gene	
Rcptr.	**Cpd.**	**pK_i**	**pEC_{50}**	**E_{max}**	**$pEC_{50}/(pK_b)$**	**E_{max}**	**$pEC_{50}/(pK_b)$**	**E_{max}**
hH_1R	HIS	3.37 ± 0.29	7.38 ± 0.05	100	6.16 ± 0.09	100	6.87 ± 0.06 [20]	100 [20]
	DPH	7.80 ± 0.17	7.82 ± 0.07	−22 ± 3	6.95 ± 0.04	−4 ± 0.1	(7.66 ± 0.24) [20]	-
hH_2R	HIS	4.32 ± 0.38	6.57 ± 0.05	100	6.94 ± 0.05	100	6.49 ± 0.27	100
	FAM	7.75 ± 0.33	7.37 ± 0.06	−10 ± 5	7.29 ± 0.10	−9 ± 0.7	7.47 ± 0.15	n.d.
hH_3R	HIS	6.80 ± 0.19	6.49 ± 0.06	100	6.47 ± 0.04	100	8.48 ± 0.09 [89]	100 [89]
	PIT	8.72 ± 0.05	7.02 ± 0.22	−21 ± 2	(8.41 ± 0.05)	-	n. d.	n. d.
hH_4R	HIS	7.25 ± 0.05	7.15 ± 0.05	100	6.40 ± 0.04	100	7.77 ± 0.12 [23]	100 [23]
	THIO	6.66 ± 0.12	7.04 ± 0.14	−45 ± 6	6.68 ± 0.04	−8 ± 1.9	6.92 ± 0.10 [23]	−32.0 ± 0.04 [23]

Competition binding (Comp. Bdg): The pKi values for histamine (HIS), diphenhydramine (DPH), famotidine (FAM), pitolisant (PIT) and thioperamide (THIO) were determined with live HEK $hH_{1-4}R$ cells in the presence of 5 nM [^{3}H]mepyramine ([^{3}H]MEP) at the hH_1R, 50 nM [^{3}H]UR-DE257 at the hH_2R, 2 nM or 5 nM [^{3}H]UR-PI294 at the hH_3R or hH_4R, respectively. **DMR:** The pEC_{50} and E_{max} values were determined by converting the DMR traces to CRCs using the positive AUC_{60} for HIS or the negative AUC_{60} for the inverse agonists (DPH at the hH_1R, FAM at the hH_2R, PIT at the hH_3R and THIO at the hH_4R). These values were subsequently normalized to AUC_{60} for the buffer (0%) and the respective highest histamine concentration (100%). The negative sign of E_{max} values for inverse agonists implies a negative deflection of the originate DMR traces (Figure 2C). All values represent means ± SEM of at least three independent experiments, each performed in triplicate. n. d. means not determined.

To the best of our knowledge, we are the first to report functional DMR data for the $hH_{2-4}Rs$, so no reference data was available. In order to compare the results, a miniG recruitment assay, recently implemented by Hoering et al. [80] for the entire HR family, was used. As the miniG recruitment assay was also performed with live HEK cells in real time, and the AUC used for data analysis, these results were particularly well suited as a reference. As a canonical alternative, a luciferase reporter gene assay was used. This assay was also performed with HEK cells but represents an endpoint measurement, in contrast to the kinetic measurements of DMR and miniG recruitment assays. Although the three assays measure different processes in the signal transduction cascade of HRs, in general, the pEC_{50} values were in good agreement, not differing more than one order of magnitude (Table 2). Exceptions are HIS at the hH_1R (DMR vs. miniG) and HIS at the hH_3R (DMR vs. luciferase). By contrast, higher discrepancies were observed regarding the efficacy of the inverse agonists. In general, inverse agonists were less efficacious in the miniG recruitment assay than in the DMR assay. However, as only one miniG protein-HR interaction was monitored rather than the holistic cellular response as in the DMR assay, this discrepancy is not surprising. A better agreement of E_{max} values was observed between the DMR and the luciferase reporter gene assay for THIO at the hH_4R.

2.3. Dissecting HIS Induced DMR Signals in HEK $hH_{1-4}R$ Cells Using G Protein Modulators

2.3.1. Impact of Individual Gα Protein Modulators on the DMR Response

As outlined above, depending on the HR subtype, different intensities and time courses of the DMR responses were observed when HEK $hH_{1-4}R$ cells were stimulated with HIS at increasing concentrations (Figure 2A). We investigated whether the receptor-specific DMR response was exclusively the result of an activation of the primary Gα protein dependent signaling pathway described in the literature (Figure 1B), or whether additional G proteins were involved in the HIS-induced DMR response. The contribution of endogenously expressed Gα proteins was analyzed using G protein pathway modulators FR900359 (FR), pertussis toxin (PTX), and cholera toxin (CTX; mechanisms for all three outlined in Figure 5A). CRCs were recorded for HIS in HEK $hH_{1-4}R$ cells in the absence and presence of CTX, PTX (both at concentrations of 1.00, 10.0 and 100 ng/mL) and FR (at concentrations of 0.01, 0.10 and 1.00 µM). In every experiment, HEK $hH_{1-4}R$ cells stimulated with HIS without (w/o) modulators served as 100% control. DMR traces recorded at the highest histamine concentration in the absence and presence of the respective modulator were compared (Figure 5B) and, as before, AUC_{60} CRCs were constructed (Supplementary Figure S10). The corresponding E_{max} and pEC_{50} values are summarized in supplementary Figure S11.

- hH_1R

Because the $G\alpha_{q/11}$ pathway is considered canonical for the hH_1R [56,57], a strong decline of the DMR response was expected upon incubating the HEK hH_1R cells with the $G\alpha_{q/11}$ modulator FR. When HEK hH_1R cells were treated with 1.00 µM FR, the time course of the DMR signal for HIS was noticeably altered, but not with 0.01 µM or 0.1 µM FR (5B green traces). In the former case, no maximum was observed and the DMR response was slower. However, even the highest FR concentration of 1.00 µM was not sufficient to eradicate the HIS DMR response (Figure 5B, green traces), although the E_{max} value was reduced to 41 ± 9.5% (Figure 6A). Likewise, Lieb et al. were also not able to completely suppress the HIS induced DMR in HEK293T-CRE-Luc-hH_1R-hMSR1 cells in the presence of 1.00 or 10.0 µM FR [20]. For comparison, a concentration of 1.00 µM FR was enough to completely disrupt the DMR response of the muscarinic M_3R, which solely couples to $G\alpha_{q/11}$ [44]. Thus, we conclude that the failure to completely suppress the DMR signal was not due to insufficient FR concentration, but rather that the residual signal in HEK hH_1R cells comes from additional (G) protein interactions. The significantly reduced pEC_{50} in the presence of 1.00 µM FR (6.81 ± 0.15) could be caused by inactivation of the $G\alpha_{q/11}$ protein abolishing the $G\alpha_{q/11}$ positive modulation, an effect seen when the G protein stabilizes the active conformation of the receptor [24,90].

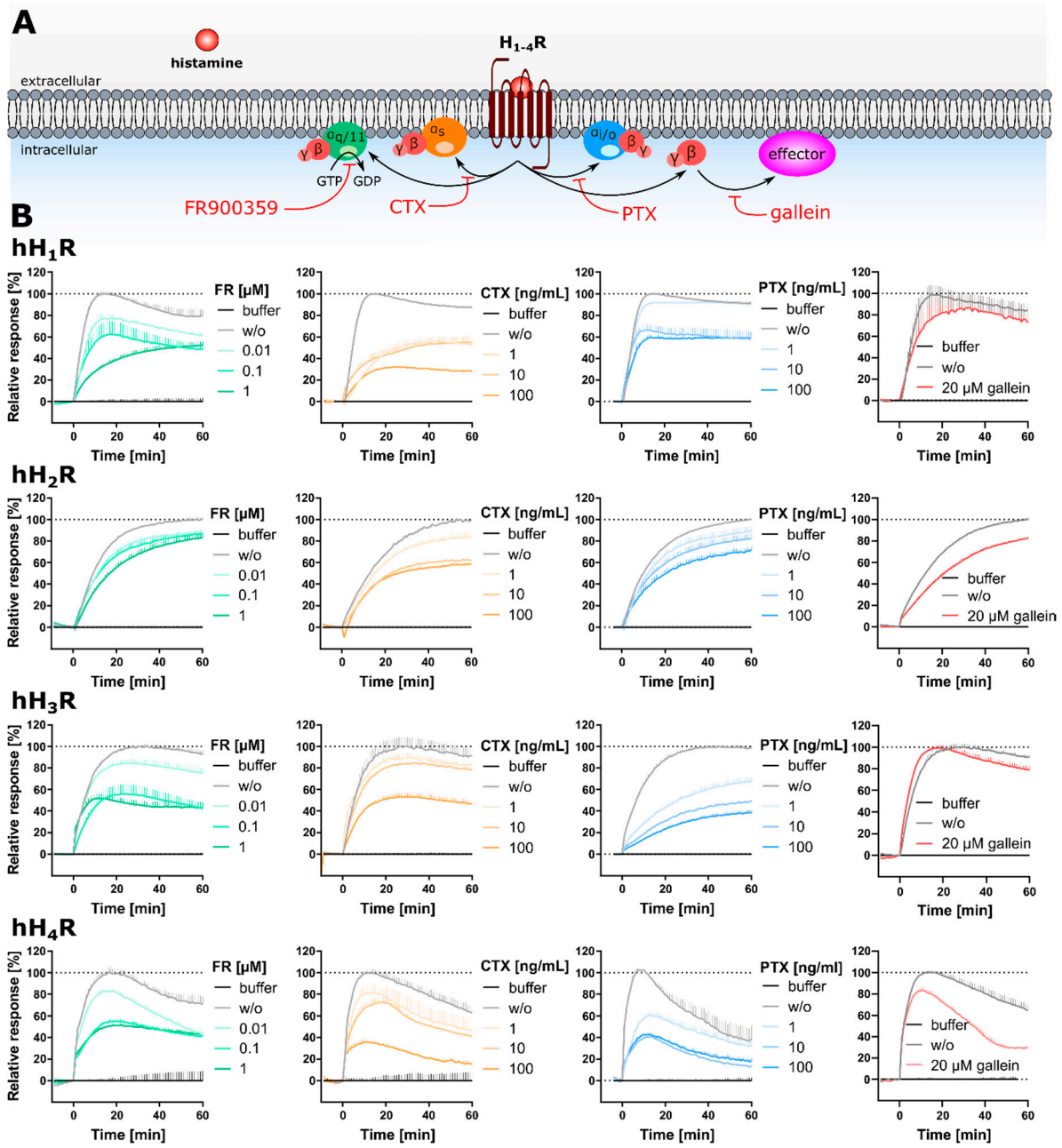

Figure 5. Effect of individual G protein modulators on the HIS induced DMR traces recorded in HEK $hH_{1-4}R$ cells. (**A**) Interference of the G protein modulators FR, CTX, PTX and gallein with histamine receptor mediated signaling. FR (alias UBO-QIC) selectively silences $G\alpha_{q/11}$ signaling by blocking the GDP-release at concentrations 0.1 to 1.0 µM [18,41,44–47]. PTX selectively and irreversibly silences $G\alpha_{i/o}$ at a concentration of 100 ng/mL by ADP-ribosylation at the Gα-subunit [20,33,37,40–42]. CTX locks the $G\alpha_s$ protein in its GTP bound state by irreversible ADP-ribosylation leading to a permanent activation of the $G\alpha_s$ protein, which is in turn uncoupled and no longer available for the GPCR [31–33,37,43] at a concentration of 100 ng/mL [31,32,37]. As this approach only masks the $G\alpha_s$ protein coupled pathway the results should be interpreted with caution. Gallein (gal) is reported to reversibly bind to the Gβγ subunit (K_d = 422 nM) [92], preventing an interaction with effector proteins [92–94]. (**B**) Representative time courses of the HIS induced DMR response in HEK $hH_{1-4}R$ cells pre-treated with G protein modulator at the indicated concentrations overnight (PTX and CTX) or 30 min (FR and gallein) before measurement of stimulation with HIS ($hH_{1,2,4}R$ at 10 µM HIS, hH_3R at 100 µM HIS). All traces were buffer-corrected and normalized to the maximum DMR response (wavelength shift in pm) of the untreated control (w/o). Data are presented as mean ± SEM of a technical triplicate.

Surprisingly, masking of the $G\alpha_s$ signaling pathway with CTX had a greater effect on the DMR response of the hH_1R (Figure 5B, orange traces) than FR. Even the lowest concentration of 1.00 ng/mL CTX enormously altered both the maximum amplitude, and the time course of the HIS induced DMR response. In this case, the DMR response was slowed down and showed no signal maximum as observed for untreated HEK hH_1R cells. An increase in CTX concentration to 100 ng/mL further reduced the signal amplitude and led to a deceleration of the DMR signal. Unexpectedly, among the investigated modulators, 100 ng/mL CTX had the strongest effect on E_{max} at the hH_1R lowering the value to 23 ± 4.9% (Figure 6A), suggesting that the $G\alpha_s$ protein is involved in the hH_1R mediated DMR signal. Indeed, it has been shown that the hH_1R can functionally interact with the $G\alpha_s$ protein in HEK cells overexpressing both the receptor and the $G\alpha_s$ protein [60,91]. The inhibition of $G\alpha_s$ pathway led to a significant increase in the pEC_{50} value (7.87 ± 0.19; Figure 6B). It is possible that the uncoupling of $G\alpha_s$ may have enhanced $G\alpha_q$ protein interaction with the hH_1R, or $G\alpha_s$ may even act as a negative modulator at hH_1R. Further investigations are necessary to determine the mechanism involved.

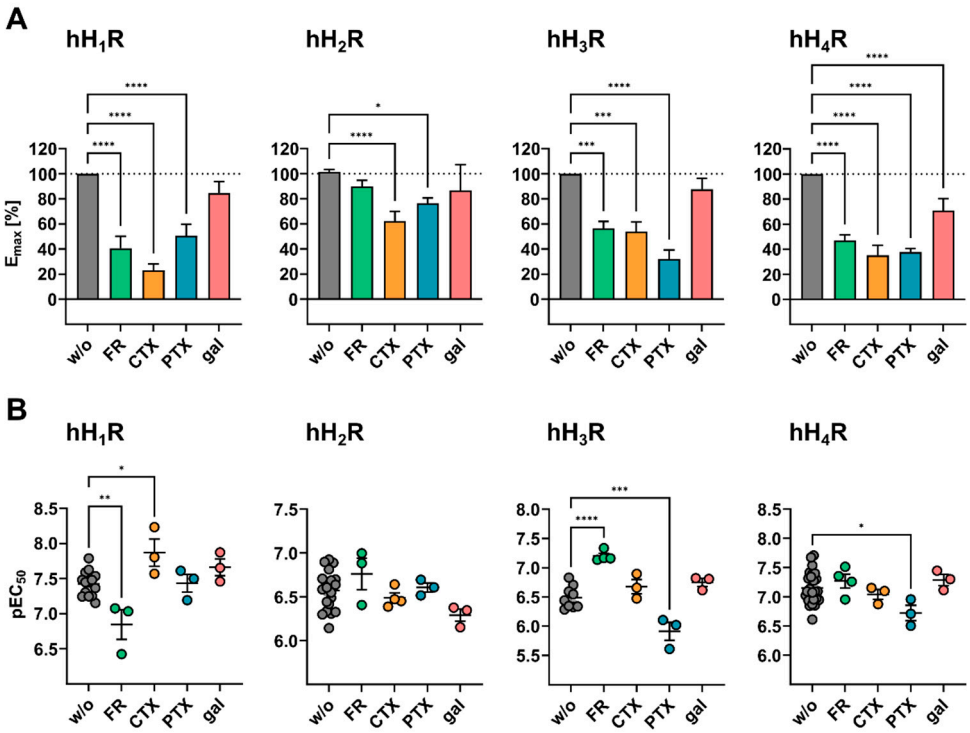

Figure 6. Effect of individual G protein modulators on the efficacy and potency of HIS at $hH_{1-4}Rs$. E_{max} and pEC_{50} values were determined for HIS in the absence and the presence of G protein modulators. (**A**) Bar chart of E_{max} values determined for HIS in absence (w/o, grey) and presence of FR (green, 1 µM), CTX (orange, 100 ng/mL), PTX (blue, 100 ng/mL) and gal (red, 20 µM). The E_{max} values were calculated using AUC_{60} at the highest HIS concentration (10 µM for $hH_{1,2,4}R$ and 100 µM for hH_3R) and normalized to the AUC_{60} of the untreated control (100%) and buffer (0%) values. (**B**) Scatter plot of the pEC_{50} values in absence (grey) and presence of G protein modulators at the concentration stated above. The pEC_{50} were determined by plotting the AUC_{60} against the respective HIS concentration. (**A**,**B**) Data presented are means ± SEM of at least three independent experiments, each performed in triplicate. Statistical difference relative to the control was analyzed by one-way ANOVA followed by Dunnett's multiple comparison test. Significance levels are indicated by asterisks (* $p \leq 0.05$, ** $p \leq 0.01$, *** $p \leq 0.001$, **** $p \leq 0.0001$).

The inhibition of $G\alpha_{i/o}$ signaling pathway with PTX reached its maximum effect at a concentration of 10.0 ng/mL at the hH_1R (Figure 5B, blue traces). Except for decreasing the signal amplitude to maximum 50 ± 9.3% of E_{max} relative to control cells (Figure 6A), PTX

had no effect on the time course of the DMR signal, suggesting $G\alpha_{i/o}$ protein involvement in hH_1R signal transduction. This is in good accordance with the literature [20,59,61]. For example, Lieb et al. showed that the hH_1R also signals via $G\alpha_{i/o}$ in the DMR assay using HEK293T-CRE-Luc-hH_1R-hMSR1, as the DMR signal was completely abolished by 100 ng/mL PTX [20].

- hH_2R

Pretreatment of HEK hH_2R cells with increasing CTX concentrations led to a gradual decrease in the signal amplitude relative to the untreated control, but, in contrast to HEK hH_1R cells, did not alter the shape of the DMR time course (Figure 5B, orange traces). At 100 ng/mL CTX, 62 ± 7.7% of the hH_2R signal was retained; a significant effect, but not as pronounced as with the other three HR subtypes (Figure 6A; hH_1R 23 ± 4.9%, hH_3R 54 ± 7.6% and hH_4R 35 ± 7.9% signal retention). This was unexpected, as the hH_2R is commonly considered as a $G\alpha_s$-coupled receptor [56,95]. Furthermore, 100 ng/mL CTX have been shown to almost completely abolish the agonist induced DMR response of the $G\alpha_s$-sensitive β_2 adrenoreceptor (β_2R) expressed by different cell types endogenously or heterologously [31,32,37]. Moreover, the pEC_{50} value of HIS remained unaffected by the treatment with CTX (Figure 6B). We expected that uncoupling of the $G\alpha_s$ protein with CTX would negatively affect the pEC_{50} value of HIS, as was the case with hH_1R after the $G\alpha_{q/11}$ protein was inactivated by FR. These data suggest that additional signaling pathways contribute to the DMR response in HEK hH_2R cells.

Apart from $G\alpha_s$, it is known that the $G\alpha_{q/11}$ protein can play a considerable role in H_2R signal transduction, dependent on the cellular background [56]. This was not confirmed in the DMR assay as the $G\alpha_{q/11}$ modulator FR was almost completely ineffective, even at a concentration of 1.00 µM (Figure 5B green traces). Although a stepwise decline of the DMR response was observed with increasing PTX concentrations to investigate the involvement of $G\alpha_{i/o}$ in the HIS induced DMR (Figure 5B blue traces), the effect was less pronounced than with CTX (E_{max} = 77 ± 4.2% at 100 ng/mL PTX versus E_{max} = 62 ± 7.7%; Figure 6A). Strikingly, in contrast to the other three HR subtypes, the individual modulators FR, CTX and PTX, had little effect on the HIS induced DMR response in HEK hH_2R cells. Two explanations can be considered. Firstly, silencing of one pathway may have caused the hH_2R to switch to other pathways, indicating promiscuous signal transduction of the receptor. Secondly, these results may also indicate the involvement of other effectors, e.g., $G\alpha_z$ or $G\alpha_{12/13}$ [59], in the hH_2R mediated DMR response.

- hH_3R

As expected, inhibition of the $G\alpha_{i/o}$ signaling pathway with PTX in HEK hH_3R cells had a dramatic impact on the DMR response to 100 µM HIS, for both the E_{max} and pEC_{50} values. Even 1.00 ng/mL of PTX was sufficient to decelerate the hH_3R DMR response (Figure 5A, blue traces) and to reduce the E_{max} to 63 ± 14% (Figure 6A), roughly a 4× more reduction than for $hH_{1,2}Rs$. However, we failed to completely suppress the signal, as at 100 ng/mL PTX 32 ± 7.2% of E_{max} remained. By contrast, Shi et al. described that the HIS response was disrupted by 100 ng/mL of PTX in a CRE-driven luciferase activity assay using HEK cells stably expressing the hH_3R [42]. Moreover, for other $G\alpha_{i/o}$ coupled receptors, e.g., the muscarinic M_2 [48], or prostaglandin $CRTH_2$ [37], PTX at a concentration of 100 ng/mL was sufficient to completely disrupt the DMR signal in CHO or HEK cells. Thus, we expect that 100 ng/mL PTX was sufficient to inactivate $G\alpha_{i/o}$ mediated signaling and conclude that other (G) proteins were involved in the hH_3R mediated DMR response. The pEC_{50} values declined with increasing PTX concentrations from 6.49 ± 0.06 (control) to 5.75 ± 0.17 and 5.91 ± 0.15 (10.0 and 100 ng/mL of PTX, respectively; Figure 6B). As described above, a similar phenomenon was observed for the hH_1R when its canonical $G\alpha_{q/11}$ signaling pathway was blocked with 1 µM FR. We believe the same hypothesis to be true here, namely that the $G\alpha_{i/o}$ protein stabilizes an active conformation of the hH_3R, resulting in decreased pEC_{50} values when blocked. Consistent with literature [57], this suggests that the $G\alpha_{i/o}$ protein plays a major role in hH_3R mediated signal transduction.

However, as it was not possible to completely abrogate the DMR response with PTX, other G protein (in)dependent signaling pathways might be involved as well.

The $G\alpha_{q/11}$ modulator FR at increasing concentrations had no effect on the time course of the HIS induced DMR response, but did decrease the signal amplitude (Figure 5B, green traces). A decrease in E_{max} to about 95 ± 5.3% was observed in the presence of 0.01 µM FR, whereas 0.10 µM FR significantly reduced the E_{max} value to 60 ± 6.4%. A ten-fold increase in FR concentration to 1.00 µM decreased the E_{max} by only additional 3% compared with 0.10 µM FR, indicating that at the latter concentration of FR the $G\alpha_{q/11}$ dependent DMR was almost completely inhibited in HEK hH_3R cells (Figure 6A). Strikingly, the pEC_{50} value was significantly increased to 7.20 ± 0.05 after treatment with 1.00 µM FR referring to the pEC_{50} of 6.49 ± 0.06 in control cells (Figure 6B). We did not expect this impact of $G\alpha_{q/11}$ inhibition because hitherto the hH_3R has been described as a $G\alpha_{i/o}$ selective receptor and to date, no evidence has been provided that the hH_3R is capable of activating a Gα protein other than $G\alpha_{i/o}$ [91].

Masking the $G\alpha_s$ signaling with CTX did not affect the time course of the HIS-induced hH_3R mediated DMR response elicited by HIS, but again the signal amplitude was affected (Figure 5B). The E_{max} values decreased to 77 ± 9.0% or 76 ± 6.3% after treatment with 1.00 or 10.0 ng/mL of CTX, respectively and was significantly reduced to 54 ± 7.61% in the presence of 100 ng/mL CTX compared to control cells (Figure 6A). In comparison, the E_{max} value at the hH_1R was already reduced to 43 ± 9.5% at a concentration of 1 ng/mL of CTX. Therefore, we reason that $G\alpha_s$ is not as involved in signal transduction at the hH_3R as at the hH_1R. This assumption was further supported by the fact that the pEC_{50} value was not significantly affected by the treatment with CTX (Figure 6B).

- hH_4R

Pre-incubation of HEK hH_4R cells with PTX at increasing concentrations to block the $G\alpha_{i/o}$ protein had no influence on the time course but did affect the signal amplitude of the HIS induced DMR response (Figure 5B). Similar to the hH_3R response, even at 1 ng/mL PTX the E_{max} was lowered to 51 ± 6.8% (Figure 6A). However, we failed to completely displace the HIS induced DMR response at the hH_4R by PTX, even at a concentration of 100 ng/mL (Figure 6A; E_{max} = 38 ± 2.9%). Elsewhere, in a luciferase reporter gene assay with HEK293-EBNA cells transfected with the hH_4R (referred to as GPRv53), 100 ng/mL PTX completely abolished the HIS induced response [96]. However, unlike the hH_3R response, an increase in PTX concentration had no effect on pEC_{50} values in HEK hH_4R cells (Figure 6B).

The contribution of the $G\alpha_s$ protein was analyzed by pre-treating the cells with CTX at increasing concentrations. Figure 5B (hH_4R orange traces) shows that the maximum responses declined stepwise, whereas time courses of the HIS induced DMR remained unaltered (Figure 5B). Only at the highest CTX concentration of 100 ng/mL, did the signal decrease substantially (E_{max} = 35 ± 7.9%; Figure 6A). Analogous to the hH_3R, we assume that $G\alpha_s$ is of smaller importance in the signal transduction of the hH_4R compared to the hH_1R, where the E_{max} value was reduced to 43 ± 9.5% with 1 ng/mL CTX. Moreover, the pEC_{50} value for HIS in HEK hH_4R cells was not affected in the presence of CTX (Figure 6B). The $G\alpha_{q/11}$ modulator FR at increasing concentrations led to a stepwise decrease in the hH_4R mediated DMR response. FR at a concentration of 0.10 µM was sufficient to decrease the DMR signal to 71 ± 18% relative to the untreated control, and a further decline was observed in the presence of 1.00 µM FR (E_{max} = 47 ± 4.5%; Figure 6A). Different to the hH_3R, the pEC_{50} value was unaltered by the blockage of the $G\alpha_{q/11}$ protein with FR (Figure 6B).

2.3.2. Impact of the Gβγ Protein Modulator Gallein on the DMR Response upon Stimulation with Histamine

In addition to Gα, the Gβγ dimer is also able to interact with effectors in the signal transduction process. A contribution of Gβγ to the DMR response was assessed by means of the small modulatory molecule gallein [92–94]. Pretreatment of HEK $hH_{1-3}R$ cells with

20 μM gallein prior to stimulation with HIS led only to a marginal reduction of the E_{max} value to approximately 85% compared to control cells (Figure 5B, red traces and Figure 6A). In the case of the hH_4R, the same gallein concentration significantly reduced the E_{max} value to 71 ± 9.3%. The pEC_{50} value for HIS remained unaltered by the treatment with gallein (Figure 6B). The modulatory effect of gallein on E_{max} values was markedly weaker at $hH_{1–4}Rs$ than for individual Gα modulators (1.00 μM FR, 100 ng/mL CTX and 100 ng/mL PTX). This may indicate that the endogenous Gβγ subunit plays a minor role in $hH_{1–4}Rs$ signal transduction in the DMR assay. Previous investigations using the cAMP-sensitive luciferase reporter gene assay with $hH_{1,2}Rs$ stably expressed in HEK293T cells also showed gallein as ineffective at reducing signal response (hH_1R [20] or hH_2R [97]). Unfortunately, to the best of our knowledge, comparable investigations with gallein concerning $hH_{3,4}Rs$ expressed in HEK cells were not available. Lavenus et al. [45] came to a similar conclusion when investigating the effect of 20 μM gallein on the Angiotensin II-induced response in HEK293-AT_1R cells using the label-free surface plasmon resonance (SPR) technique. Further experiments are therefore necessary to clarify the involvement of Gβγ dimer in the signal transduction mediated by the $hH_{1–4}Rs$.

2.3.3. Impact of Gα Protein Modulator Combinations on the Histamine Induced DMR Response

None of the four HR subtypes displayed completely suppressed DMR signals with single G protein modulators (Figure 6A). These results prompted us to investigate whether a complete inhibition of the DMR signal in HEK $hH_{1–4}R$ cells is achievable by combining the Gα protein modulators PTX, CTX and FR. At this point it should be noted that PTX and CTX were used at a concentration of 10.0 ng/mL instead of 100 ng/mL to avoid off target effects, which was usually sufficient to achieve the maximum effect (Supplementary Figure S11). HEK $hH_{1–4}R$ cells were treated with indicated modulators prior to stimulation with 10 μM HIS (Figure 7).

In HEK hH_1R cells, each of the modulator combinations changed the time course of the HIS induced DMR response (Figure 7A), consistent with results from experiments with individual modulators (Figure 5B). Substantial depression of E_{max} to 14 ± 8.4% was seen in HEK hH_1R cells after pretreatment with a combination of PTX and CTX (Figure 7B), corroborating with our previous results for the individual contributions of $G\alpha_{s/i/o}$. A stronger reduction of the signal was observed when combining either PTX or CTX with FR, where the signal was reduced almost to the basal level (E_{max}(PTX + FR) = 3.4 ± 3.5%, E_{max}(CTX + FR) = 5.7 ± 0.8%; Figure 7B). The DMR signal was completely removed with a combination of the three modulators (PTX, CTX and FR). Therefore, we hypothesize that the HIS induced DMR response observed in HEK hH_1R cells were exclusively transmitted via the three main classes of G proteins, namely $G\alpha_{q/11}$, $G\alpha_s$ and $G\alpha_{i/o}$ proteins.

In accordance with the observations on individually applied Gα protein modulators (Figure 6), none of the modulator combinations altered the time course of the DMR response in HEK hH_2R cells (Figure 7A). Surprisingly, the HIS induced DMR response in HEK hH_2R cells was not even reduced by half upon treatment with a triple modulator combination (E_{max} (CTX, PTX, FR) = 55 ± 2.2%). In supplementary Figure S11, we showed that for both PTX and CTX, increasing the concentration from 10 ng/mL to 100 ng/mL no longer significantly reduced the DMR signal at the hH_2R and FR had no effect on the E_{max} value at hH_2R. Thus, we can exclude that PTX and CTX at a concentration of 10 ng/mL might not have been sufficient to completely inhibit the respective signaling pathways. Beyond this, at the $hH_{1,3,4}Rs$, the same modulator combination caused a more pronounced decrease in the E_{max} value (Figure 7). Both arguments suggest that the weak impact of the triple modulator combination on the E_{max} was a hH_2R-specific phenomenon. We conclude that in HEK hH_2R cells the $G\alpha_{q/11}$, $G\alpha_s$ and $G\alpha_{i/o}$ are not mainly responsible for the HIS induced DMR response, opposed to the $hH_{1,3,4}Rs$. Referring to the aforementioned hypotheses constructed from the individually applied modulators, it appears that the hH_2R is not only promiscuous with these Gα proteins, but there is also growing evidence for a possible

interaction of hH_2R with the $G\alpha_{12/13}$ and/or $G\alpha_z$, which are endogenously expressed in HEK cells [62].

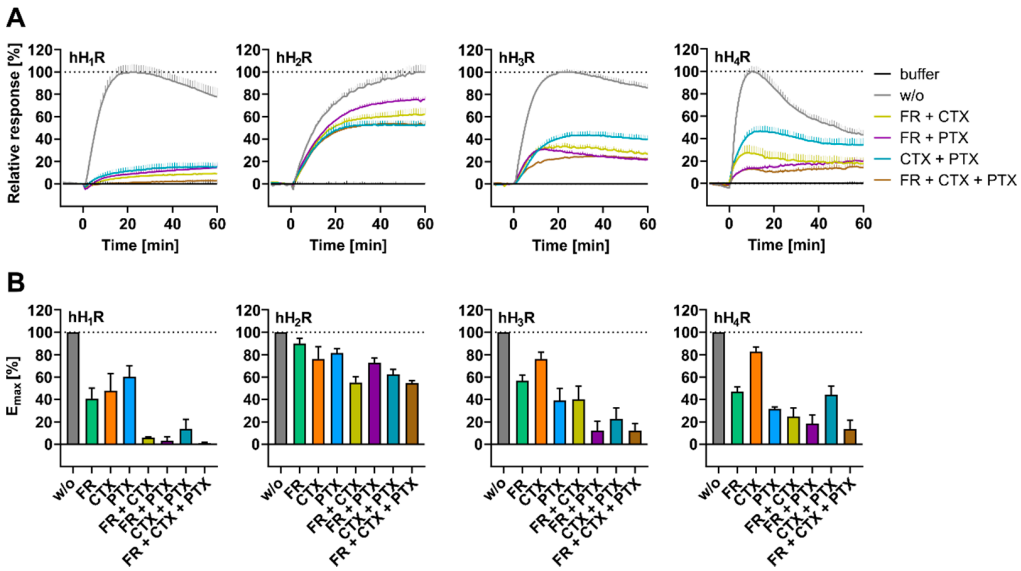

Figure 7. Impact of a combined application of Gα protein modulators FR, CTX and PTX on the DMR response at $hH_{1-4}R$. (**A**) Representative DMR traces recorded for HIS in the absence (w/o) and in the presence of Gα protein modulators FR (1 μM, 30 min before measurement), CTX and/or PTX (both 10 ng/mL overnight) in HEK $hH_{1-4}R$ cells. (**B**) The AUC_{60} was calculated for the traces and normalized to the AUC_{60} of the untreated control (10 μM HIS without (w/o) modulator (100%) and to the AUC_{60} of the buffer control (0%). The values represent mean ± SEM of three independent experiments each performed in triplicate.

In experiments with individually applied Gα modulators, a marked deceleration of the DMR response was observed in HEK hH_3R cells in the presence of 10 ng/mL PTX (Figure 5B). As expected, such a retardation of the DMR signal was observed when HEK hH_3R cells were pre-treated with modulator combinations comprising 10 ng/mL of PTX (Figure 7A). Unexpectedly, a combination of 1 μM FR + 10 ng/mL of CTX decelerated the DMR response. Moreover, the same combination (FR + CTX) markedly reduced the E_{max} to 40 ± 12% (Figure 7B). Both the impact on the time courses and the reduced E_{max} value in the presence of FR + CTX suggest that $G\alpha_{q/11}$ and $G\alpha_s$ are involved in the hH_3R mediated DMR response. However, in comparison, a stronger decrease in E_{max} value was observed when combining 1 μM FR with 10 ng/mL of PTX to jointly inhibit $G\alpha_{q/11}$ and $G\alpha_{i/o}$ signaling pathways. This modulator combination reduced the E_{max} to 12 ± 8.3%, reaching a plateau that was found to be non-suppressible by the triple modulator combination of FR + CTX + PTX (E_{max} = 12 ± 6.4%; Figure 7B) suggesting that $G\alpha_{i/o}$ and $G\alpha_{q/11}$ played a more pronounced role in the hH_3R mediated DMR response to HIS than $G\alpha_s$. Again, as with the hH_2R, the HIS induced DMR response was not completely ablated by the triple modulator combination. Inter alia, one possible explanation for this might be an involvement of additional G proteins such as $G\alpha_{12/13}$ and/or $G\alpha_z$. However, it should be noted that, unlike for the $hH_{1,2}Rs$, the concentration of CTX in the triple modulator combination (FR + CTX + PTX) is a factor to be considered. In experiments with CTX alone (Supplementary Figure S11), 10 ng/mL CTX were not sufficient to achieve the maximum effect. Precisely, in the presence of 10 ng/mL an E_{max} value of 76 ± 6.3% was obtained, whereas 100 ng/mL CTX reduced the E_{max} value to 54 ± 7.6%. Although this difference was not determined to be significant (one-way ANOVA analysis followed by Tukey's multiple comparison test; $p = 0.1980$), we still find it worth mentioning.

Likewise, we examined the influence of modulator combinations on the DMR signal in HEK hH_4R cells. We would like to note that the differences in E_{max} values between the

different modulator combinations were subtly nuanced rather than clear, just as with the individual modulators in Section 2.3.1. None of the Gα modulators effected the time courses of the HIS induced DMR responses when applied individually (Figure 5B). However, in combination, FR + PTX and FR + CTX + PTX altered the time course of the DMR response to HIS (Figure 7A). In both cases the DMR signal showed no peak and did not decline continuously, as observed in control experiments without modulators (Figure 2A). Instead, the DMR response increased steadily over time upon stimulation with HIS (Figure 7A). We took this as a hint that $G\alpha_{q/11}$ and $G\alpha_{i/o}$ have more impact on the signal transduction of hH_4R in HEK cells than $G\alpha_s$; nevertheless, the involvement of the latter should not be neglected. This opinion was enforced when E_{max} values were considered (Figure 7B); the treatment of HEK hH_4R cells with CTX + PTX decreased the E_{max} to 44 ± 7.7%, whereas addition of FR (FR + CTX + PTX) reduced the E_{max} to a final value of 14 ± 8.0%, relative to control cells. It is also remarkable that a jointly inhibition of $G\alpha_{q/11}$ and $G\alpha_{i/o}$ signaling pathways with FR + PTX decreased the maximum response by almost the same level (E_{max} = 19 ± 7.7%) as the triple combination FR + CTX + PTX. Unexpectedly, the E_{max} value in presence of 10 ng/mL CTX + 10 ng/mL PTX was higher (E_{max} = 44 ± 7.7%) than that upon treatment with 10 ng/mL of PTX alone (E_{max} = 32 ± 1.9%). This might be due to the mechanism of action of CTX, as CTX does not directly inhibit the $G\alpha_s$ protein, but rather masks the $G\alpha_s$ dependent signaling pathway by permanent $G\alpha_s$ protein activation. Similar to the hH_3R, the inhibition of the three signaling pathways was not sufficient to completely remove the hH_4R mediated response, as 14 ± 8.0% of E_{max} remained after treatment with FR + CTX + PTX (Figure 7B). Again, as with the hH_3R, this demonstrates that signal transduction of the hH_4R overexpressed in HEK cells occurred mainly through activation of $G\alpha_{i/o}$, $G\alpha_s$ and $G\alpha_{q/11}$ proteins, but the DMR signal might also arise from either $G\beta\gamma$, $G\alpha_{12/13}$ and/or $G\alpha_Z$ proteins.

Of note, the two structurally related receptor subtypes hH_3R and hH_4R have similar coupling specificities to Gα proteins, and so it is unsurprising that so that inhibition of the corresponding Gα signaling pathways led to comparable reduction in E_{max} values.

2.4. Investigation of HIS Induced DMR Signaling in G Protein Knock Out Cells

2.4.1. Expression of $hH_{1-4}Rs$ in $\Delta G\alpha_s$ HEK Cells

In addition to the concept of classical pharmacology, namely the employment of specific G protein modulators as molecular tools to elucidate cellular processes, we explored a molecular biology approach to better understand the contribution of individual Gα isoforms to the $hH_{1-4}R$ mediated DMR response using CRISPR/Cas9 modified HEK cells devoid of distinct Gα proteins ($\Delta G\alpha_x$ HEK cells). For the generation of $\Delta G\alpha_x$ HEK $hH_{1-4}R$ cells the $\Delta G\alpha_{s/l}$ HEK [63], $\Delta G\alpha_{q/11}$ HEK [44], $\Delta G\alpha_{12/13}$ HEK [64] and $\Delta G\alpha_{six}$ HEK [41] cells were stably transfected with the pIRESneo3-SP-FLAG-$hH_{1-4}R$ constructs and used as polyclonal cell lines. We confirmed the expression of the $hH_{1-4}Rs$ in $\Delta G\alpha_x$ HEK $hH_{1-4}R$ cells by radioligand saturation binding using live cells (Supplementary Figure S3). The expression levels of $hH_{1-4}Rs$ in $\Delta G\alpha_x$ HEK $hH_{1-4}R$ cells were calculated as mentioned for HEK $hH_{1-4}R$ cells (Table 1). When comparing the expression levels of respective HR subtypes in HEK $hH_{1-4}R$ cells with those in $\Delta G\alpha_x$ HEK $hH_{1-4}R$ cells (e.g., expression of the hH_1R in HEK hH_1R versus in $\Delta G\alpha_x$ HEK hH_1R cells), we noted that the expression levels of $hH_{2-4}Rs$ were in the same range. In the case of the hH_1R, the expression level was determined to be 10-fold lower in $\Delta G\alpha_{s/l,\,q/11,\,12/13}$ HEK hH_1R cells compared to HEK hH_1R cells. On the one hand, this difference may be due to the single clone selection procedure by which only the highest response HEK hH_1R cells were obtained, thereby having the highest receptor expression level. The fact that only the binding capacity but not the affinity of the radioligand [^{3}H]MEP was affected would argue in favor of this. However, this is contradicted by the fact that no difference in expression level was observed between the single clone HEK $hH_{2-4}R$ and polyclonal $\Delta G\alpha_x$ HEK $hH_{2-4}R$ cells. On the other hand, we cannot exclude that knock-out of Gα proteins might have impaired either the expression of the hH_1R or the detection of the binding capacity of

the radioligand [^{3}H]MEP to the hH_1R in $\Delta G\alpha_x$ HEK hH_1R cells. This suspicion arose when we failed to detect the expression of the hH_1R in $\Delta G\alpha_{six}$ hH_1R cells by radioligand saturation binding (Supplementary Figure S3), although a concentration-dependent signal was detected in the DMR assay when these cells were stimulated with HIS (Section 2.4.2 and supplementary Figure S12). By contrast, no DMR signal was observed in $\Delta G\alpha_{six}$ HEK cells devoid of the hH_1R (Supplementary Figure S6), suggesting that the hH_1R was expressed in $\Delta G\alpha_{six}$ HEK hH_1R cells. For MEP, which has been reclassified as an inverse agonist [98], multiple binding sites differing in affinity and binding capacity for the H_1R have been reported [99,100]. Moreover, the intrinsic negative efficacy of MEP is thought to be due to the stabilization of a G-protein-coupled state of the H_1R that is not capable of eliciting a response [100]. Considering this, we argue in favor of the latter hypothesis, namely that the absence of Gα proteins may have affected the binding of [^{3}H]MEP to the hH_1R. However, as this research project is focused on the results in the DMR assay, we have not pursued this issue. The pK_d values determined with both HEK $hH_{1-4}R$ and $\Delta G\alpha_x$ HEK $hH_{1-4}R$ cells were in very good agreement with literature data (Table 1), except for $\Delta G\alpha_{12/13}$ hH_2R and $\Delta G\alpha_{six}$ hH_2R. In both cases, the pK_d value increased significantly to 7.98 + 0.05 ($\Delta G\alpha_{12/13}$ hH_2R, $p < 0.0001$) and 7.86 + 0.06 ($\Delta G\alpha_{six}$ hH_2R, $p = 0.0004$) relative to the value determined using HEK hH_2R cells (pK_d = 7.19 + 0.06). Apparently, the absence of $G\alpha_{12/13}$ facilitates the binding of the radioligand [^{3}H]DE-257 to the hH_2R.

The impact of Gα protein knock-out on the affinity of HIS to the $hH_{1-4}Rs$ was analyzed by radioligand competition binding with HIS as a competitor using live $\Delta G\alpha_x$ HEK $hH_{1-4}R$ cells (Figure 8 and supplementary Table S2). Of note, such experiments were not performed with $\Delta G\alpha_{six}$ HEK hH_1R, as the expression of hH_1R was not detectable in saturation binding experiments. Unfortunately, in $\Delta G\alpha_{s/l,\,q/11}$ HEK hH_1R cells a pK_i value could not be determined for HIS due to an ambiguous curve fit of the data. Although not statistically significant ($p = 0.0545$, *t*-test two-tailed), the pK_i value for HIS in $\Delta G\alpha_{12/13}$ HEK hH_1R cells ($pK_i = 2.23 \pm 0.37$) was approx. one order of magnitude lower than at HEK hH_1R cells ($pK_i = 3.37 \pm 0.29$). While the absence of $G\alpha_{s/l}$ or $G\alpha_{q/11}$ proteins in $\Delta G\alpha_{s/l,\,q/11}$ HEK hH_2R cells had no impact on the pK_i of HIS ($pK_i = 3.68 \pm 0.09$ and 4.23 ± 0.11, respectively), the value decreased approx. two-fold at $\Delta G\alpha_{six}$ HEK hH_2R cells ($pK_i = 1.82 \pm 0.28$) compared to HEK hH_2R cells ($pK_i = 4.32 \pm 0.38$). The listed discrepancy of the pK_i values of HIS at the $hH_{1,2}Rs$ were not surprising, as saturation binding experiments (Table 1) demonstrate that the absence of Gα proteins can positively or negatively impact ligand binding at the $hH_{1,2}Rs$. The pK_i values determined for HIS using $\Delta G\alpha_x$ HEK $hH_{3,4}R$ cells were in good agreement with literature data and the results determined with HEK $hH_{3,4}R$ cells (Supplementary Table S2).

2.4.2. Stimulation of $\Delta G\alpha_x$ HEK $hH_{1-4}R$ Cells in the DMR Assay with HIS

A schematic illustration of the $\Delta G\alpha_x$ HEK $hH_{1-4}R$ cells with regard to G protein knock-out is given in Figure 9A. The $\Delta G\alpha_x$ HEK $hH_{1-4}R$ cells were stimulated with HIS at increasing concentrations and the DMR response was recorded for 60 min. Throughout, the DMR traces showed a positive deflection and were concentration dependent (Figure 9B; AUC_{60} CRCs in supplementary Figure S12). By contrast, stimulation of $\Delta G\alpha_{q/11}$ HEK, $\Delta G\alpha_{12/13}$ HEK and $\Delta G\alpha_{six}$ HEK cells devoid of $hH_{1-4}Rs$ with HIS did not provoke a DMR signal. However, with $\Delta G\alpha_s$ HEK cells, devoid of a HR subtype, a slight increase in the DMR signal was observed, but only at high HIS concentrations (1.00 and 10.0 µM). Therefore, we considered this DMR increase as negligible due to its low intensity (Supplementary Figure S6). To evaluate the effect of Gα protein knock-out on the DMR response, the AUC_{60} at the respective HIS concentration ($hH_{1,2,4}Rs$ 10 µM HIS and hH_3R 100 µM HIS) using $\Delta G\alpha_x$ HEK $hH_{1-4}R$ cells was compared to the mean AUC_{60} of HEK $hH_{1-4}R$ cells, in which all G proteins were present (100% control, Figure 10). This approximation was reasonable, because mostly the expression of the different receptor subtypes was comparable (Table 1).

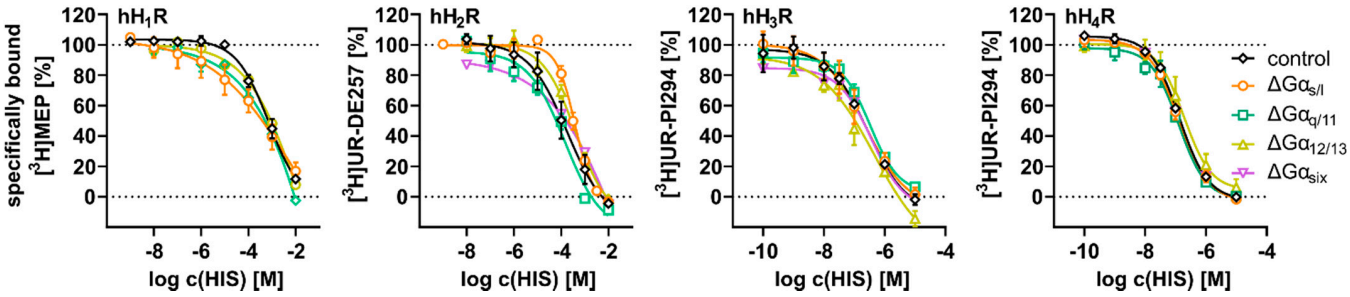

Figure 8. Radioligand displacement curves determined for histamine (HIS) at HEK $hH_{1-4}R$ and $\Delta G\alpha_x$ $hH_{1-4}R$ cells. HIS was incubated at indicated concentrations in the presence of 5 nM [^{3}H]mepyramine ([^{3}H]MEP) at the hH_1R, 50 nM [^{3}H]UR_DE257 at the hH_2R, 2 nM or 5 nM [^{3}H]UR_PI294 hH_3R or hH_4R, respectively. The non_specific binding was determined in the presence of DPH (hH_1R), FAM (hH_2R) or HIS ($hH_{3,4}Rs$), each at a final concentration of 10 µM. The non_specific binding was subtracted from the total binding to receive the specific binding. Specific binding was normalized to the buffer value (100%) and the corrected non_specific binding value (0%). Each point represents mean ± SEM of at least three independent experiments, each performed in triplicate.

When comparing the HIS induced DMR responses of $\Delta G\alpha_{s/l,\ 12/13}$ HEK hH_1R with that of HEK hH_1R cells by visual inspection, there was no discernible difference (Figure 9B). Consequently, the E_{max} values for HIS using $\Delta G\alpha_{s/l,\ 12/13}$ HEK hH_1R were not significantly different from the control cell line HEK hH_1R (Figure 10A). Of note, in Section 2.4.1 we discussed that the binding capacity of [^{3}H]MEP was by factor 10 lower in $\Delta G\alpha_x$ HEK hH_1R cells than in HEK hH_1R cells. Apparently, this difference had no impact on the signal amplitude and the E_{max} value, supporting the hypothesis that the absence of the Gα proteins impaired the binding of [^{3}H]MEP to the hH_1R [99,100]. The absence of the $G\alpha_s$ protein in $\Delta G\alpha_{s/l}$ HEK hH_1R cells caused the pEC_{50} value for HIS to significantly increase to 7.96 + 0.09 compared to HEK hH_1R cells (pEC_{50} = 7.43 + 0.05), an effect also observed in $\Delta G\alpha_{12/13}$ HEK hH_1R cells (pEC_{50} = 7.78 + 0.05). By contrast, the absence of the $G\alpha_{q/11}$ protein in $\Delta G\alpha_{q/11,\ six}$ HEK hH_1R cells lowered the signal amplitude (E_{max} = 46 ± 38%; Figure 10A) and slightly altered the time course of the signal (Figure 9B). Moreover, the pEC_{50} value for HIS in $\Delta G\alpha_{q/11,\ six}$ HEK hH_1R cells was significantly lower in both cell lines ($\Delta G\alpha_{q/11}$ HEK hH_1R pEC_{50} = 6.38 ± 0.02, $\Delta G\alpha_{six}$ HEK hH_1R pEC_{50} = 6.63 ± 0.15) than with HEK hH_1R cells (Figure 10B). We still hypothesize that the presence of $G\alpha_{q/11}$ stabilized the active state of hH_1R in HEK cells and that this effect is further enhanced in the absence of other Gα proteins.

The lack of Gα proteins in $\Delta G\alpha_x$ HEK hH_2R cells did not alter the time course of the DMR response (Figure 9B). Despite the lack of the $G\alpha_s$ protein in $\Delta G\alpha_s$ HEK hH_2R cells, stimulation with HIS evoked a robust DMR response, similar to that observed with HEK hH_2R cells. Consequently, the E_{max} value of $\Delta G\alpha_s$ HEK hH_2R cells was not significantly different compared to HEK hH_2R cells (Figure 10A). This was unexpected, as we observed a significant decrease in E_{max} in our experiments with CTX to mask $G\alpha_s$. Stimulation of $\Delta G\alpha_{q/11}$ HEK hH_2R cells with HIS showed a decrease in the E_{max} value to 84 ± 14% (Figure 10A) compared to HEK hH_2R cells. The pEC_{50} value determined for HIS in $\Delta G\alpha_{s/l,\ q/11}$ HEK hH_2R cells remained in the same range as in HEK hH_2R cells (Figure 10B). In Section 2.3.1 it was considered that $G\alpha_{12/13}$ protein might be responsible for the HIS induced DMR at HEK hH_2R cells. This hypothesis was affirmed as the signal amplitude of the DMR response to HIS in $\Delta G\alpha_{12/13}$ HEK hH_2R cells was considerably lower compared to that of HEK hH_2R cells (Figure 9B). The corresponding E_{max} value determined in $\Delta G\alpha_{12/13}$ HEK hH_2R cells amounted to 10.0 ± 0.8% (Figure 10A) relative to HEK hH_2R cells. In $\Delta G\alpha_{six}$ HEK hH_2R cells, which lack the $G\alpha_{12/13}$ protein too, the E_{max} value was also reduced significantly to 20 ± 2.0%. In addition to E_{max}, the HIS pEC_{50} value in both cell lines wassignificantly reduced ($\Delta G\alpha_{12/13}$ HEK hH_2R pEC_{50} = 5.77 ± 0.46; $\Delta G\alpha_{six}$ HEK hH_2R pEC_{50} = 6.01 ± 0.04) compared to HEK hH_2R cells (pEC_{50} = 6.57 ± 0.05; Figure 10B). We interpreted this as an indication that $G\alpha_{12/13}$ might stabilize the active

state of the hH_2R and is essential for hH_2R mediated signal transduction in HEK cells. Further studies are necessary to substantiate or rule out the involvement of other cellular constituents, such as $G\alpha_z$.

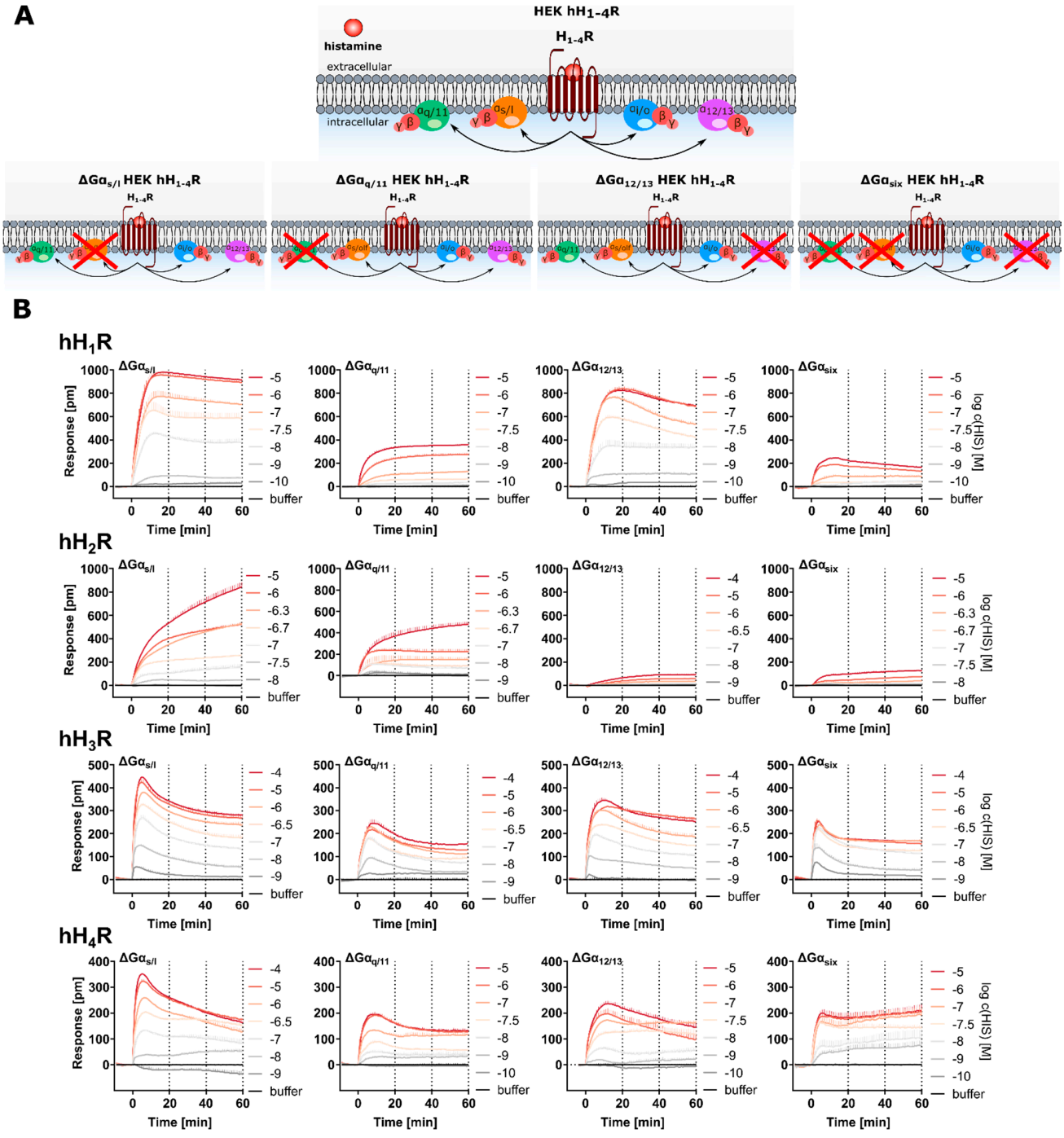

Figure 9. DMR responses recorded in Gα protein knock–out HEK $hH_{1-4}R$ cells upon stimulation with HIS. (**A**) Schematics of used Gα protein knock–out HEK ($\Delta G\alpha_x$ HEK) cells. The $\Delta G\alpha_x$ HEK cells lacking either the $G\alpha_{s/l}$ ($\Delta G\alpha_{s/l}$ HEK) [63], the $G\alpha_{q/11}$ ($\Delta G\alpha_{q/11}$ HEK) [44], the $G\alpha_{12/13}$ ($\Delta G\alpha_{12/13}$ HEK) [64] or six Gα proteins ($\Delta G\alpha_{s/l,\ q/11,\ 12/13}$ = $\Delta G\alpha_{six}$ HEK) [41] were stably transfected with $hH_{1-4}Rs$. The knocked–out Gα protein is marked with a red "X". HEK $hH_{1-4}R$ cells, expressing all four G protein classes were used as reference. (**B**) The $\Delta G\alpha_x$ HEK $hH_{1-4}R$ cells either lacking the $G\alpha_{s/l}$ ($\Delta G\alpha_{s/l}$), $G\alpha_{q/11}$ ($\Delta G\alpha_{q/11}$), $G\alpha_{12/13}$ ($\Delta G\alpha_{12/13}$) or $G\alpha_{s/l,\ q/11,\ 12/13}$ ($\Delta G\alpha_{six}$) proteins were stimulated with indicated HIS concentration and the DMR response was recorded for 60 min. Depicted are representative DMR traces, which were corrected for the buffer. Each trace represent mean ± SEM of a representative experiment performed in triplicate.

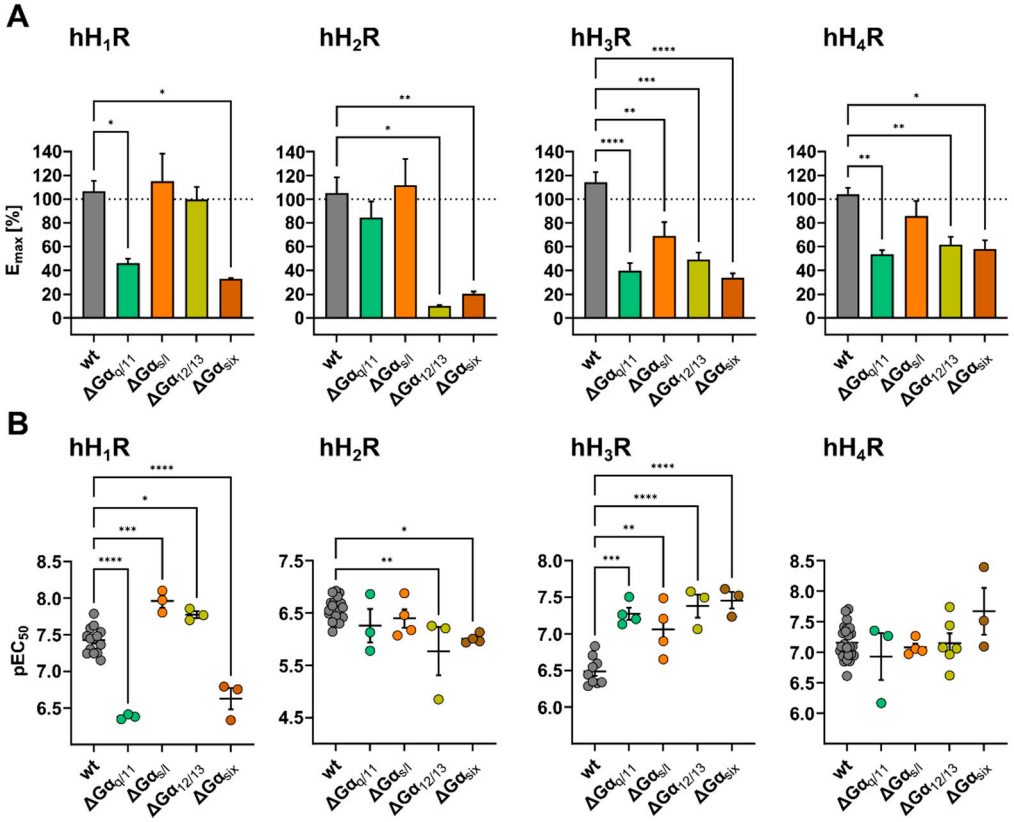

Figure 10. Effect of G protein knock-out on the efficacy and potency of HIS at $hH_{1-4}Rs$. E_{max} and pEC_{50} values determined for HIS in $\Delta G\alpha_x$ HEK $hH_{1-4}R$ cells. (**A**) Bar chart of E_{max} values determined for HIS in HEK $hH_{1-4}R$ cells (wt, grey) and in $\Delta G\alpha_{s/l}$ HEK, $\Delta G\alpha_{q/11}$ HEK, $\Delta G\alpha_{12/13}$ HEK, $\Delta G\alpha_{six}$ HEK cells each stably expressing $hH_{1-4}Rs$, respectively. The E_{max} max values were calculated using AUC_{60} at the highest HIS concentration (10 µM for $hH_{1,2,4}R$ and 100 µM for hH_3R) and normalized to the mean AUC_{60} from HEK $hH_{1-4}R$ cells at the corresponding receptor subtype (100%) and to the corresponding buffer value (0%) determined in $\Delta G\alpha_x$ HEK $hH_{1-4}R$ cells. (**B**) Scatter plot of the pEC_{50} values in HEK $hH_{1-4}R$ cells (wt, grey) and in $\Delta G\alpha_{s/l}$ HEK, $\Delta G\alpha_{q/11}$ HEK, $\Delta G\alpha_{12/13}$ HEK, $\Delta G\alpha_{six}$ HEK cells each stably expressing $hH_{1-4}Rs$, respectively. The pEC_{50} were determined by plotting the AUC_{60} against the respective HIS concentration. (**A**,**B**) Data presented are means ± SEM of at least three independent experiments each performed in triplicate. Statistical difference relative to the control was analyzed by one-way ANOVA followed by Dunnett's multiple comparison test. Significance levels are indicated by asterisks (* $p \leq 0.05$, ** $p \leq 0.01$, *** $p \leq 0.001$, **** $p \leq 0.0001$).

Unlike HEK hH_3R cells (all G proteins present) in which the DMR signal increased steadily but slowly after addition of HIS (Figure 2A), the DMR signal in all $\Delta G\alpha_x$ HEK hH_3R cells increased rapidly, showing a peak within 10 min upon stimulation with HIS (Figure 9B). Interestingly, such a time course was not observed in any of the experiments in HEK hH_3R cells with Gα protein modulators (Figure 5B). The E_{max} values of HIS in $\Delta G\alpha_{q/11}$ HEK hH_3R, $\Delta G\alpha_{12/13}$ HEK hH_3R cells and $\Delta G\alpha_{s/l}$ HEK hH_3R cells significantly declined to 40 ± 6.4%, 49 ± 5.5% and 69 ± 11%, respectively, compared to the 100% control (HEK hH_3R cells; Figure 10A). In $\Delta G\alpha_{six}$ HEK cells, the $G\alpha_{q/11,\, s/l,\, 12/13}$ proteins were knocked-out, so it can be assumed that among the common Gα proteins, only the $G\alpha_{i/o}$ was expressed. Upon stimulation of these cells with HIS, a weaker DMR response was detected with an E_{max} value of 34 ± 3.7% compared to HEK hH_3R cells (Figure 10A). As the $G\alpha_{i/o}$ signaling pathway is almost exclusively considered as physiologically relevant for the hH_3R, we did not expect a complete suppression of the signal in $\Delta G\alpha_{six}$ HEK hH_3R cells. However, before assigning this response solely to the $G\alpha_{i/o}$ protein, it should be noted that other G proteins, such as $G\alpha_z$ should be considered. Strikingly, the pEC_{50} value

determined for HIS in all $\Delta G\alpha_x$ HEK hH_3R cells was significantly higher (Figure 10B) compared to that determined with HEK hH_3R cells.

Different to the hH_3R, the time course of the HIS induced DMR response recorded using $\Delta G\alpha_x$ hH_4R cells (Figure 9) agreed well with that of HEK hH_4R cells (100% control). The lack of $G\alpha_{q/11}$ in $\Delta G\alpha_{q/11}$ HEK hH_4R cells led to a significant decrease in the DMR signal to 54 ± 3.3% (Figure 10A), whereas knock-out of $G\alpha_s$ ($\Delta G\alpha_s$ HEK hH_4R) showed a weaker impact on the DMR response, reducing the E_{max} to 86 ± 13% relative to the control. This was surprising because a much more pronounced suppression was observed after treatment with CTX. In $\Delta G\alpha_{12/13}$ HEK hH_4R cells, the E_{max} value was suppressed to 62 ± 6.7% compared to HEK hH_4R cells; therefore, it can be concluded that the $G\alpha_{12/13}$ pathway seems to be involved in the signal transduction of the hH_4R in HEK cells. The knock-out of the three subclasses of Gα proteins in $\Delta G\alpha_{six}$ hH_4R cells reduced the E_{max} value to 58 ± 7.3% compared to HEK hH_4R cells, being in good agreement with results determined with the $G\alpha_{i/o}$ modulator PTX. However, as the other three G proteins classes have been shown to be essentially involved in the signaling of the hH_4R (see Section 2.3.1), we expected a more pronounced reduction of the signal. Perhaps the cells compensate for the lack of targeted G proteins by enhanced expression of either $G\alpha_{i/o}$ or other (G) proteins are involved in the signal transduction process.

2.5. Pharmacological versus Molecular Biological Approach to Silence Gα Protein

The contribution of Gα proteins to the DMR response elicited by HIS at the $hH_{1-4}Rs$ stably expressed in HEK cells was investigated either by a classical pharmacological (G protein modulators) or by a molecular biological (Gα protein knock-out) approach. In the pharmacological approach, HEK $hH_{1-4}Rs$ cells were pre-treated with Gα protein modulators FR, CTX and PTX to silence either $G\alpha_{q/11}$, $G\alpha_s$ or $G\alpha_{i/o}$ proteins, respectively (Section 2.3). In the molecular biological approach, the $G\alpha_{q/11}$, $G\alpha_s$, $G\alpha_{12/13}$ proteins were knocked out individually or in combination (knock-out of $G\alpha_{q/11,\,s/l,\,12/13}$) using the CRISPR/Cas9 technology (Section 2.4). The focus of this section was to highlight the similarities and discuss the differences of the results obtained with these two approaches.

Silencing of the $G\alpha_{q/11}$ signaling pathway either by 1.00 µM FR in HEK $hH_{1-4}R$ cells or by knocking out $G\alpha_{q/11}$ in $\Delta G\alpha_{q/11}$ HEK $hH_{1-4}R$ cells have shown agreement in terms of E_{max} and pEC_{50} values for HIS. At the hH_1R, for example, the time course of DMR traces were similarly altered by both approaches compared to the control (HEK hH_1R cell w/o; Figure 11) and the E_{max} for HIS was significantly reduced ($\Delta G\alpha_{q/11}$ HEK hH_1R E_{max} = 46 ± 3.8; HEK hH_1R + 1 µM FR E_{max} = 41 ± 9.5) relative to HEK hH_1R cells (100% w/o modulator). Moreover, both procedures to silence the $G\alpha_{q/11}$ have led to a significant decrease in the pEC_{50} determined for HIS ($\Delta G\alpha_{q/11}$ HEK hH_1R pEC_{50} = 6.38 ± 0.02; HEK hH_1R + 1 µM FR pEC_{50} = 6.60 ± 0.29) relative to HEK hH_1R control cells (pEC_{50} = 7.43 ± 0.05). A similar effect was observed for HIS with $\Delta G\alpha_{six}$ HEK hH_1R cells, which also lack the $G\alpha_{q/11}$ protein. We expected such a pronounced perturbation of the E_{max} and the pEC_{50} value, as hH_1R is predominantly described as a $G\alpha_{q/11}$ coupled receptor [57]. It was surprising that for the hH_2R, silencing of the $G\alpha_{q/11}$ signaling pathway by both approaches (FR and $G\alpha_{q/11}$ knock-out) had almost no impact on the DMR response (kinetics, E_{max} and pEC_{50}), as it is commonly accepted that the $G\alpha_{q/11}$ protein is considerably involved in the signal transduction of the hH_2R [56]. We cannot confirm this in the DMR assay using HEK cells. By contrast, deactivation of the $G\alpha_{q/11}$ signaling pathway either by FR or knock-out affected the E_{max} value for HIS at $hH_{3,4}Rs$ (Figure 11). In HEK $hH_{3,4}Rs$, 1.00 µM FR reduced the E_{max} to 57 ± 5.4% and 47 ± 4.5%, respectively (Figure 6A) and in $\Delta G\alpha_{q/11}$ HEK $hH_{3,4}R$ cells the E_{max} was diminished to 40 ± 6.4% and 54 ± 3.3%, respectively (Figure 10A; compared to untreated HEK $hH_{3,4}R$ cells). Moreover, at hH_3R, the pEC_{50} value for HIS increased significantly by both approaches (HEK hH_3R + 1 µM FR pEC_{50} = 7.20 ± 0.05, $\Delta G\alpha_{q/11}$ HEK hH_3R cells pEC_{50} = 7.28 ± 0.08) relative to HEK hH_3R cells (pEC_{50} = 6.49 ± 0.06). By contrast, in both systems the pEC_{50} determined for HIS at the hH_4R was not significantly altered. As both

approaches led to the same consequences, we are convinced that the results are not an artifact and conclude that $G\alpha_{q/11}$ contributed to the DMR signaling of the $hH_{3,4}Rs$ in HEK cells, even though the limited literature suggests the opposite [91,101]. We consider this as an intriguing starting point for further investigations.

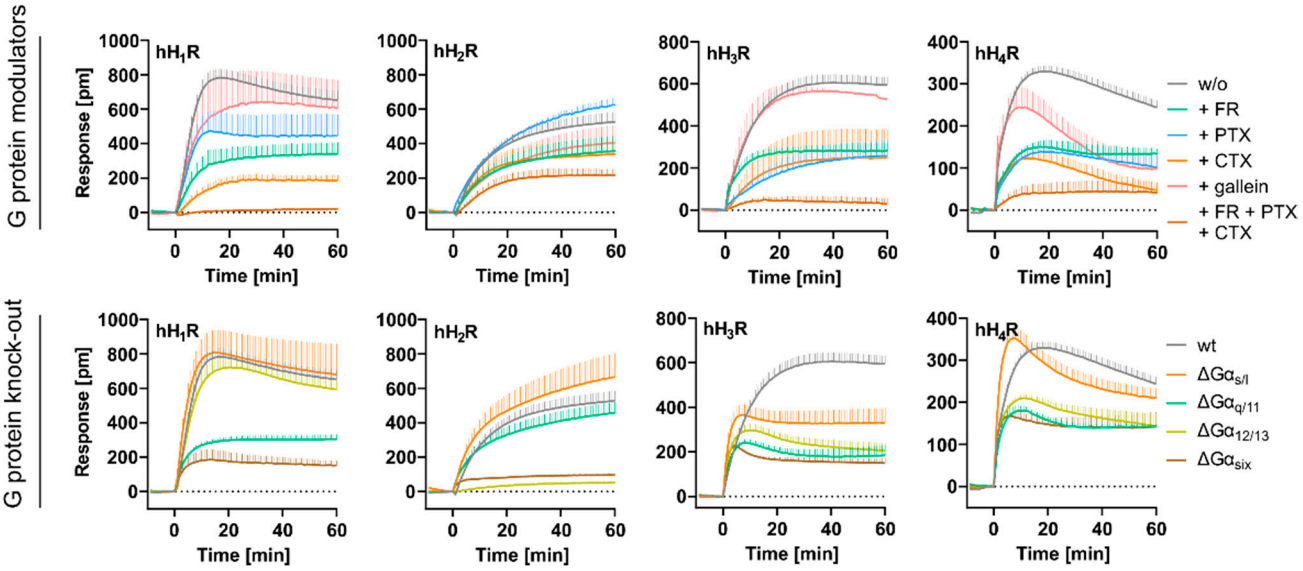

Figure 11. G protein inhibition using a classical pharmacological concept (G protein modulator) or by a molecular biological approach (Gα protein knock-out cells). DMR traces recorded for HIS in HEK $hH_{1-4}R$ cells in the absence (w/o modulator) or presence of G protein modulators (100 ng/mL PTX, 100 ng/mL CTX, 1 µM FR, 20 µM gallein (gal) and combination of 10 ng/mL PTX + 10 ng/mL CTX + 1 µM FR) or in Gα protein knock-out cells ($\Delta G\alpha_{s/l}$ HEK, $\Delta G\alpha_{q/11}$ HEK, $\Delta G\alpha_{12/13}$ HEK and $\Delta G\alpha_{six}$ HEK cells) stably transfected with $hH_{1-4}Rs$. In the case of the $hH_{1,2,4}Rs$ the cells were stimulated with 10 µM HIS, whereas in the case of the hH_3R the cells were stimulated with 100 µM HIS. All traces shown were corrected for the assay buffer and represent means ± SEM of at least three independent experiments, each performed in triplicate.

Unlike $G\alpha_{q/11}$, we found differences between CTX and knocking-out $G\alpha_s$ (Figure 11). To be more specific, in experiments using HEK $hH_{1-4}Rs$ cells pre-treated with 100 ng/mL CTX, we concluded that $G\alpha_s$ was markedly involved in the $hH_{1-4}R$ mediated signal transduction process in HEK cells throughout. For example, for the hH_1R the E_{max} was dramatically reduced to 23 ± 4.9% (Figure 6A). Moreover, the E_{max} of HIS determined in HEK $hH_{3,4}R$ cells was significantly reduced to 54 ± 7.6% or 35 ± 7.9%, respectively (Figures 5 and 6A). By contrast, we observed that knock-out of $G\alpha_{s/l}$ in $\Delta G\alpha_{s/l}$ HEK $hH_{1-4}R$ cells had a weaker effect on the E_{max} value. In $\Delta G\alpha_{s/l}$ HEK $hH_{1,3,4}R$ cells, the E_{max} value amounted to 115 ± 23%, 69 ± 12% and 86 ± 13% of control responses respectively (Figure 10A), suggesting that $G\alpha_s$ plays a supporting role in the HIS induced DMR response. Various explanations can be considered to address this discrepancy in E_{max} between the two approaches. On the one hand, it seems possible that HEK cells have "adapted" their repertoire of expressed Gα proteins to compensate for the lack of $G\alpha_s$ in $\Delta G\alpha_{s/l}$ HEK $hH_{1-4}R$ cells so that the E_{max} remained unaffected. On the other hand, it is conceivable that, in addition to $G\alpha_s$, CTX may have off-target effects that were relevant for the generation of the DMR signal in HEK $hH_{1-4}R$ cells, which led to a decrease in E_{max}. Elucidation of the difference in results between the pharmacological and molecular biological approaches for $G\alpha_s$ modulation should be pursued in the future.

Regarding the $G\alpha_{i/o}$ signaling pathway, in the experiments with PTX we found that $G\alpha_{i/o}$ was directly involved in the hH_1R mediated DMR response in HEK cells, as the E_{max} was reduced to 50 ± 9.3% in the presence of 100 ng/mL PTX (Figure 6A). Alternatively, in $\Delta G\alpha_{six}$ hH_1R cells, which among the canonical Gα proteins only express $G\alpha_{i/o}$, HIS elicited a DMR response with a corresponding E_{max} of 33 ± 0.5% (Figure 10A). As we ruled out that $G\alpha_{12/13}$ and $G\alpha_z$ play a role in the hH_1R mediated DMR response (Figure 7), we conclude

that the residual 33% represent the interaction of the hH_1R with the $G\alpha_{i/o}$, in accordance with literature [57]. The $hH_{3,4}Rs$ are considered as $G\alpha_{i/o}$ selective receptors [57], however, according to our experiments, we conclude that $G\alpha_{i/o}$ was not exclusively involved in the manifestation of the DMR signal in HEK $hH_{3,4}R$ cells. Namely, pretreatment of HEK $hH_{3,4}R$ cells with 100 ng/mL of PTX led to a dramatic decrease in E_{max}, and the pEC_{50} was reduced in HEK hH_3R cells compared to controls (Figure 6B). Additionally, in the presence of the $G\alpha_{q/11}$ protein modulator FR, the E_{max} was significantly reduced for both receptor subtypes (Figure 6B). Moreover, it was not possible to completely abolish the HIS triggered DMR in HEK $hH_{3,4}R$ cells with a modulator cocktail comprising FR, CTX and PTX (Figure 7). In addition to the canonical Gα proteins, we observed that the $G\alpha_{12/13}$ proteins might be involved in the signal transduction process of the $hH_{3,4}Rs$, as the E_{max} in $\Delta G\alpha_{12/13}$ HEK $hH_{3,4}R$ cells decreased by about 55% compared with HEK $hH_{3,4}R$ cells (Figure 10A). However, we cannot exclude that the $G\alpha_z$ might also be involved. In the case of the hH_2R, the modulation of $G\alpha_{i/o}$ by 100 ng/mL PTX had a weaker effect on the HIS induced DMR response (E_{max} = 77 ± 4.1%) compared to the $hH_{1,3,4}Rs$ (E_{max} 51–32%; Figure 6A). Moreover, we failed to suppress the HIS induced DMR response by more than 40% with Gα protein modulators FR, CTX and PTX (Figure 7), and most of the DMR signal was abolished in $\Delta G\alpha_{12/13}$ HEK hH_2R and $\Delta G\alpha_{six}$ HEK hH_2R cells, both of which lack the $G\alpha_{12/13}$ protein (Figure 10A). We conclude that $G\alpha_{q/11}$, $G\alpha_s$, and $G\alpha_{i/o}$ played a minor role in the generation of the HIS DMR signal in HEK hH_2R cells, and that $G\alpha_{12/13}$ proteins must have been involved. It has already been described in the literature that the hH_2R is capable to interact with the $G\alpha_{12/13}$ protein [59,60], however, it was unexpected that the involvement of $G\alpha_{12/13}$ would exceed the contribution of $G\alpha_{q/11}$, $G\alpha_s$, and $G\alpha_{i/o}$.

In summary, we successfully established a DMR assay for the entire histaminergic receptor family stably expressed in HEK cells, providing an opportunity to monitor the functions of HRs and its ligands in real-time. High S/B-ratios above 100 for HIS and 24 for inverse agonists facilitate investigations on signaling pathways of $hH_{1–4}Rs$ and might be beneficial for further investigations, e.g., with respect to inverse agonism and functional bias of HR ligands. We took advantage of the integrative nature of the DMR assay to investigate the involvement of endogenously expressed G proteins in the signaling transduction processes mediated by $hH_{1–4}Rs$. However, in view of the physiological relevance of the results, experiments with cells or tissues which endogenously express the receptors are pending. For example, using modulatory tools such as PTX, CTX and FR, the impact of ligands on the signaling pathway of the receptor can be studied as well, which is particularly interesting with respect to ligand induced signal bias. At this point, it should be noted that apart from G proteins, the recruitment of β-arrestin also plays an important role in the signal transduction processes of GPCRs [24] and consequently also for HRs [102–104]. Interestingly, although investigations on the mechanistic details of β-arrestin activation are available, there is also evidence that no β-arrestin mediated signaling was observed in absence of functional G proteins [41]. The DMR assay could be a valuable approach to investigate the contribution of β-arrestins to a holistic response of HRs. Pharmacological tools (e.g., biased ligands, protein inhibitors) in combination with a molecular biological approach (e.g., cells lacking (either) Gα proteins and/or β-arrestins) might be helpful to gain new insights into the interaction of G proteins and β-arrestins [41]. Moreover, several polymorphisms were discovered for HRs [105] which are under investigation to be associated with diseases such as heart failure (H_2R [106]) or allergic rhinitis (H_4R [107]) and correlated with the effectiveness of drugs (H_1R [108], H_3R [109], H_4R [110]). Thus, the DMR assay might be a valuable tool to characterize such polymorphisms of HRs, especially focusing on the differences in the signaling pathways between receptor variants.

Although our studies still leave some open questions, we are convinced that the presented work provides valuable information for further investigation on signal transduction mechanisms of the HR family.

3. Materials and Methods

3.1. Materials

Dulbecco's modified Eagle's medium with phenol red (DMEM), L-glutamine solution (200 mM) and penicillin-streptomycin solution (10,000 units penicillin and 10 mg streptomycin per mL in 0.9% NaCl) were purchased from Sigma-Aldrich (Taufkirchen, Germany). Hanks' Balanced Salt Solution (HBSS) and Leibovitz' L-15 medium (L-15) were from Fisher Scientific (Nidderau, Germany). FBS, and geneticin (G418) were from Merck Biochrom (Darmstadt, Germany). Trypsin/EDTA was either from Merck Biochrom (Darmstadt, Germany) or from VWR International GmbH (Ismaning, Germany). The pIRESpuro3 vector was a gift from Prof. Dr. Gunter Meister (Biochemistry I, University of Regensburg, Regensburg, Germany). Histamine dihydrochloride (HIS), was from Fisher Scientific (Schwerte, Germany). Diphenhydramine hydrochloride (DPH), mepyramine maleate (MEP) and famotidine (FAM) were from Sigma (Taufkirchen, Germany). Thioperamide maleate (THIO), UR-DE257 (DE257) and JNJ7777120 (JNJ) were synthesized in-house according to standard procedures. Pitolisant hydrochloride (PIT) was kindly provided by Prof. Dr. Katarzyna Kiec-Kononowicz (Jagiellonian University, Krakow, Poland). The ligands were dissolved in Millipore water, except for famotidine (FAM), which was dissolved in DMSO (Merck, Darmstadt, Germany). FR900359 (UBO-QIC) was purchased from the Institute of Pharmaceutical Biology, University of Bonn (Bonn, Germany). Pertussis Toxin (PTX) was purchased from Bio-Techne GmbH (Wiesbaden, Germany) and Cholera Toxin from Enzo Life Sciences (Lörrach, Germany). Gallein was from Santa Cruz Biotechnology (Heidelberg, Germany).

3.2. Cell Culture

3.2.1. Parental Cells and General Culture Conditions

HEK293T cells were a kindly provided by Prof. Dr. Wulf Schneider (Institute for Medical Microbiology and Hygiene, Regensburg, Germany). HEK293T and CRISPR/Cas9 edited HEK293A lacking the Gα proteins $G\alpha_s$ + $G\alpha_{olf}$ ($\Delta G\alpha_{s/l}$ HEK) [63], $G\alpha_q$ + $G\alpha_{11}$ ($\Delta G\alpha_{q/11}$ HEK) [44], $G\alpha_{12}$ + $G\alpha_{13}$ ($\Delta G\alpha_{12/13}$ HEK) [64] or $G\alpha_q$ + $G\alpha_{olf}$ + $G\alpha_{11}$ + $G\alpha_s$ + $G\alpha_{12}$ + $G\alpha_{13}$ ($\Delta G\alpha_{six}$ HEK) [41] were maintained in DMEM supplemented with 10% FBS, penicillin (100 U/mL) and streptomycin (100 µg/mL) (P/S) at 37 °C in a water-saturated atmosphere containing 5% CO_2. Cells were periodically monitored for mycoplasma contamination by means of the Venor GeM Mycoplasma Detection Kit (Minerva Biolabs, Berlin, Germany) and proven negative.

3.2.2. Generation of HEK $hH_{1-4}R$ Cells

The HEK hH_1R, HEK hH_2R, HEK hH_3R and HEK hH_4R cells are abbreviated designations of the previously described stable single clone transfectants: HEK293T-SP-FLAG-hH_1R K12 [111], HEK293T-SP-FLAG-hH_2R K46 [111], HEK293T-SP-FLAG-hH_3R K16 [89] and HEK293T-SP-FLAG-hH_4R K3 cells [89], respectively. The procedures for molecular cloning of the receptors and the generation of the stable cell lines are described elsewhere [89,111]. The cells were cultured in DMEM supplemented with 10% FBS + P/S and 600 µg/mL G418.

3.2.3. Generation of $\Delta G\alpha_x$ HEK $hH_{1-4}R$ Cells

For the generation of $\Delta G\alpha_x$ HEK $hH_{1-4}R$ cells CRISPR/Cas9 modified HEK293A cells lacking the Gα proteins $G\alpha_s$ + $G\alpha_{olf}$ ($\Delta G\alpha_{s/l}$ HEK) [63], $G\alpha_q$ + $G\alpha_{11}$ ($\Delta G\alpha_{q/11}$ HEK) [44], $G\alpha_{12}$ + $G\alpha_{13}$ ($\Delta G\alpha_{12/13}$ HEK) [64] or $G\alpha_q$ + $G\alpha_{olf}$ + $G\alpha_{11}$ + $G\alpha_s$ + $G\alpha_{12}$ + $G\alpha_{13}$ ($\Delta G\alpha_{six}$ HEK) [41] were transfected with the pIRESneo3-SP-FLAG vector encoding the $hH_{1-4}Rs$ according to the procedure described for HEK hH_4R cells [89] except that no single clone selection was performed. The cells were cultured in DMEM supplemented with 10% FBS + P/S and 600 µg/mL G418.

3.3. Methods

3.3.1. Radioligand Binding

All radioligand binding experiments (saturation and competition) were performed using suspensions of live HEK $hH_{1-4}R$ and $\Delta G\alpha_x$ HEK $hH_{1-4}R$ cells. The cells were cultivated in DMEM supplemented with 10% FBS + P/S and 600 µg/mL G418 until 90–100% confluency was reached. On the day of the assay, the cells were detached by trypsinization (0.05% trypsin, 0.02% EDTA in PBS, at 37 °C for 2–4 min), harvested by centrifugation (800× *g* at rt for 5 min) and resuspended in L-15 medium devoid of additional supplements. The number of cells was determined using a hemocytometer (Neubauer, improved) and the cell density was adjusted to 1.0×10^6 cells/mL.

Before dispensing the cell suspension, all (radio)ligand dilutions were prepared 10-fold concentrated in L-15 medium and dispensed (10 µL/well) in 96 well plates (PP microplates, Greiner Bio-One, Frickenhausen, Germany). Total binding was determined in the presence of L-15 medium (10 µL/well), and the non-specific binding was assessed in the presence of a competitor: for hH_1R diphenhydramine (DPH), for hH_2R famotidine (FAM), for $hH_{3,4}Rs$ histamine (HIS), each at a final concentration of 10 µM. For saturation binding experiments, serial dilutions of the following radioligands were prepared (10 µL/well): [^{3}H]MEP (a_s = 20 Ci/mM, Hartmann Analytics GmbH, Braunschweig, Germany) for the hH_1R, [^{3}H]UR-DE257 (a_s = 32.9 Ci/mmol) [69] for the hH_2R and [^{3}H]UR-PI294 (a_s = 93.3 Ci/mmol) [70] for the $hH_{3,4}Rs$. For competition binding experiments, dilutions of "cold" ligands (10 µL/well) were incubated in the presence of 5 nM [^{3}H]MEP for the hH_1R, 50 nM [^{3}H]UR-DE257 for the hH_2R, 2 nM [^{3}H]UR-PI294 for the hH_3R and 5 nM [^{3}H]UR-PI294 for the hH_4R.

Subsequently, the cell suspension was added to the (radio)ligands (80 µL/well) to reach a final assay volume of 100 µL/well. After an incubation period of 60–120 min, the cells were harvested by filtration using a Brandel 96 sample harvester and the radioactivity was determined by liquid scintillation counting as described previously [112].

Data was analyzed using the GraphPad Prism 8 or 9 software (San Diego, CA, USA). Specific binding was calculated by subtracting the non-specific binding from the total binding. For saturation binding experiments binding data was plotted against the free radioligand concentration (nM) and best fitted to a one site saturation binding model (one site—total and non-specific binding; one site—specific binding) yielding K_d values. Receptor expression was quantified using the extrapolated B_{max} values, specific activity (a_s) of the radioligands and the cell number seeded per well and is indicated as specific binding sites per cell.

For competition binding experiments, the specific binding was plotted against the −log(concentration ligand) and analyzed applying the four parameters logistic equation (log(modulator) vs. response—variable slope (four parameters)) yielding the pIC_{50} values, which were individually converted to pKi values using the Cheng–Prusoff equation [113].

3.3.2. DMR Assay

The DMR assay was essentially performed as described [38] with the following modifications: The cells were cultured in DMEM supplemented with 10% FBS, 2 mM L-glutamine, P/S, and 600 µg/mL G418 until 90–100% confluency. The day before the assay, the cells were detached by trypsinization (0.05% trypsin, 0.02% EDTA in PBS, at 37 °C for 2–4 min), harvested by centrifugation (800× *g*, RT, 5 min,) and subsequently resuspended in DMEM supplemented with 10% FBS + P/S w/o G418. The cell density was adjusted to 1×10^6 cells/mL and the cell suspension was dispensed (90 µL/well) into an uncoated label-free 96 well plate (Cat. No. 5080, Corning B.V. Life Sciences, Amsterdam, Netherlands). Subsequently, the cells were spun down at 600× *g* for 1 min and allowed to attach in a humidified atmosphere containing 5% CO_2 at 37 °C overnight. On the day of the measurement, the cells were gently washed twice with assay medium (HBSS containing 20 mM HEPES). After the last washing step, the final volume was adjusted to 90 µL/well with assay medium and the plate was centrifuged at 600× *g* for 1 min. The

cells were allowed to equilibrate at 37 °C for at least 2 h in an EnSpire multimode plate reader (PerkinElmer, Rodgau, Germany), before the baseline was recorded every minute for 5–10 min. Immediately after the baseline record, the compounds (10 µL/well; 10-fold concentrated in assay medium) were added and the response was recorded every minute for 60 min.

For experiments with the G-protein modulators PTX and CTX the cells were pretreated with the modulator at the respective final concentration (1.00, 10.0 or 100 ng/mL) overnight and the assay was performed as described above. In the case of FR900359 and gallein the cells were incubated with the modulator (FR900359 1.00, 0.10 or 0.01 µM; gallein 20.0 µM) for 30 min before the baseline record. Afterwards the assay was performed by analogy with the procedure described above.

The time course data is presented as resonance wave-length shift in pm relative to the last data point before the test compounds were added at time zero. Data were analyzed using the GraphPad Prism 8 and 9 software (San Diego, CA, USA). For analysis, the data were corrected for the baseline drift by subtracting the mean values of the buffer control. Subsequently, the area under curve (AUC) was calculated individually for each well defining the first 5–10 values as baseline. For the estimation of the S/B ratios the modulus of the AUC was used according to the following equation.

$$\frac{S}{B}\text{ratio} = \frac{\left|AUC_{signal}\right|}{\left|AUC_{buffer}\right|}$$

Corresponding to the signal deflection (positive or negative) the positive or the negative AUC was used for the construction of concentration response curves. The AUCs were normalized to the maximum response elicited by the highest histamine concentration (100% control) and assay medium (0% control) and plotted against the logarithmic ligand concentration. The pEC_{50} values were calculated by applying the four parameters logistic equation (log(agonist) vs. response—variable slope (four parameters)). Real-time DMR traces are presented from representative experiments (mean ± SEM) with each trace reflecting the average of three technical replicates. Each experiment was performed at least three times to obtain at least three independent biological replicates.

3.4. Statistical Analyses

Statistical differences were analyzed using either the student *t* test (two-tailed) or one-way ANOVA followed by Dunnett's or Tukey's multiple comparisons test, as indicated in the corresponding Figures/Tables. All calculated *p*-values are two-sided and considered as statistically significant when lower than 0.5 indicated as * $p \leq 0.05$, ** $p \leq 0.01$, *** $p \leq 0.001$, **** $p \leq 0.0001$. All calculations were performed using the GraphPad Prism 8 or 9 software (San Diego, CA, USA).

Supplementary Materials: The following supplementary Materials are available online at https://www.mdpi.com/article/10.3390/ijms22189739/s1.

Author Contributions: Conceptualization, U.S.-E. and G.B.; methodology, U.S.-E. and N.P.; validation, U.S.-E.; formal analysis, U.S.-E.; investigation, U.S.-E. and N.P.; resources, A.I., G.B. and A.S.; data curation, U.S.-E.; writing—original draft preparation, U.S.-E.; writing—review and editing, U.S.-E., N.P., A.I., G.B. and A.S.; visualization, U.S.-E.; supervision, G.B. and A.S.; project administration, U.S.-E.; funding acquisition, A.S. All authors have read and agreed to the published version of the manuscript.

Funding: This work was supported by the Graduate Training Program GRK 1910 of the Deutsche Forschungsgemeinschaft (A.S.). A.I. was funded by the PRIME 19gm5910013, the LEAP 20gm0010004 and the BINDS JP20am0101095 from the Japan Agency for Medical Research and Development (AMED); KAKENHI 21H04791 from the Japan Society for the Promotion of Science (JSPS).

Institutional Review Board Statement: Not applicable.

Informed Consent Statement: Not applicable.

Data Availability Statement: The data presented in this study are available on request from the first author.

Acknowledgments: We are grateful to Maria Beer-Krön, Valerie Huber and Bettina Brechenmacher for excellent technical assistance. We are grateful to Laura Humphrys for proofreading and editing the manuscript. Moreover, we want to thank Lukas Grätz and Timo Littmann for their scientific expertise in the generation of the HEK $hH_{1-4}R$ cells.

Conflicts of Interest: The authors declare no conflict of interest. The funders had no role in the design of the study; in the collection, analyses, or interpretation of data; in the writing of the manuscript, or in the decision to publish the results.

References

1. Katritch, V.; Cherezov, V.; Stevens, R.C. Structure-function of the G protein-coupled receptor superfamily. *Annu. Rev. Pharmacol. Toxicol.* **2013**, *53*, 531–556. [CrossRef]
2. Hauser, A.S.; Attwood, M.M.; Rask-Andersen, M.; Schioth, H.B.; Gloriam, D.E. Trends in GPCR drug discovery: New agents, targets and indications. *Nat. Rev. Drug Discov.* **2017**, *16*, 829–842. [CrossRef] [PubMed]
3. Milligan, G.; Kostenis, E. Heterotrimeric G-proteins: A short history. *Br. J. Pharm.* **2006**, *147* (Suppl. 1), S46–S55. [CrossRef] [PubMed]
4. Kristiansen, K. Molecular mechanisms of ligand binding, signaling, and regulation within the superfamily of G-protein-coupled receptors: Molecular modeling and mutagenesis approaches to receptor structure and function. *Pharmacol. Ther.* **2004**, *103*, 21–80. [CrossRef] [PubMed]
5. Smrcka, A.V. G protein betagamma subunits: Central mediators of G protein-coupled receptor signaling. *Cell Mol. Life Sci.* **2008**, *65*, 2191–2214. [CrossRef] [PubMed]
6. Khan, S.M.; Sleno, R.; Gora, S.; Zylbergold, P.; Laverdure, J.P.; Labbe, J.C.; Miller, G.J.; Hebert, T.E. The expanding roles of Gbetagamma subunits in G protein-coupled receptor signaling and drug action. *Pharm. Rev.* **2013**, *65*, 545–577. [CrossRef]
7. Hur, E.M.; Kim, K.T. G protein-coupled receptor signalling and cross-talk: Achieving rapidity and specificity. *Cell Signal.* **2002**, *14*, 397–405. [CrossRef]
8. Smith, J.S.; Lefkowitz, R.J.; Rajagopal, S. Biased signalling: From simple switches to allosteric microprocessors. *Nat. Rev. Drug Discov.* **2018**, *17*, 243–260. [CrossRef] [PubMed]
9. Seyedabadi, M.; Ghahremani, M.H.; Albert, P.R. Biased signaling of G protein coupled receptors (GPCRs): Molecular determinants of GPCR/transducer selectivity and therapeutic potential. *Pharmacol. Ther.* **2019**, *200*, 148–178. [CrossRef]
10. Lefkowitz, R.J. Historical review: A brief history and personal retrospective of seven-transmembrane receptors. *Trends Pharmacol. Sci.* **2004**, *25*, 413–422. [CrossRef]
11. Zhao, P.; Furness, S.G.B. The nature of efficacy at G protein-coupled receptors. *Biochem. Pharmacol.* **2019**, *170*, 113647. [CrossRef]
12. Zhang, R.; Xie, X. Tools for GPCR drug discovery. *Acta. Pharm. Sin* **2012**, *33*, 372–384. [CrossRef] [PubMed]
13. Miyano, K.; Sudo, Y.; Yokoyama, A.; Hisaoka-Nakashima, K.; Morioka, N.; Takebayashi, M.; Nakata, Y.; Higami, Y.; Uezono, Y. History of the G protein-coupled receptor (GPCR) assays from traditional to a state-of-the-art biosensor assay. *J. Pharm. Sci.* **2014**, *126*, 302–309. [CrossRef]
14. Yasi, E.A.; Kruyer, N.S.; Peralta-Yahya, P. Advances in G protein-coupled receptor high-throughput screening. *Curr. Opin. Biotechnol.* **2020**, *64*, 210–217. [CrossRef] [PubMed]
15. Schihada, H.; Vandenabeele, S.; Zabel, U.; Frank, M.; Lohse, M.J.; Maiellaro, I. A universal bioluminescence resonance energy transfer sensor design enables high-sensitivity screening of GPCR activation dynamics. *Commun. Biol.* **2018**, *1*, 105. [CrossRef]
16. Wan, Q.; Okashah, N.; Inoue, A.; Nehme, R.; Carpenter, B.; Tate, C.G.; Lambert, N.A. Mini G protein probes for active G protein-coupled receptors (GPCRs) in live cells. *J. Biol. Chem.* **2018**, *293*, 7466–7473. [CrossRef] [PubMed]
17. Misawa, N.; Kafi, A.K.M.; Hattori, M.; Miura, K.; Masuda, K.; Ozawa, T. Rapid and High-Sensitivity Cell-Based Assays of Protein−Protein Interactions Using Split Click Beetle Luciferase Complementation: An Approach to the Study of G-Protein-Coupled Receptors. *Anal. Chem.* **2010**, *82*, 2552–2560. [CrossRef] [PubMed]
18. Littmann, T.; Ozawa, T.; Hoffmann, C.; Buschauer, A.; Bernhardt, G. A split luciferase-based probe for quantitative proximal determination of Galphaq signalling in live cells. *Sci. Rep.* **2018**, *8*, 17179. [CrossRef]
19. Werner, K.; Neumann, D.; Buschauer, A.; Seifert, R. No evidence for histamine H4 receptor in human monocytes. *J. Pharmacol. Exp. Ther.* **2014**, *351*, 519–526. [CrossRef]
20. Lieb, S.; Littmann, T.; Plank, N.; Felixberger, J.; Tanaka, M.; Schafer, T.; Krief, S.; Elz, S.; Friedland, K.; Bernhardt, G.; et al. Label-free versus conventional cellular assays: Functional investigations on the human histamine H1 receptor. *Pharmacol. Res.* **2016**, *114*, 13–26. [CrossRef]
21. Bakker, R.A.; Casarosa, P.; Timmerman, H.; Smit, M.J.; Leurs, R. Constitutively active Gq/11-coupled receptors enable signaling by co-expressed G(i/o)-coupled receptors. *J. Biol. Chem.* **2004**, *279*, 5152–5161. [CrossRef]

22. Bongers, G.; Sallmen, T.; Passani, M.B.; Mariottini, C.; Wendelin, D.; Lozada, A.; Marle, A.; Navis, M.; Blandina, P.; Bakker, R.A.; et al. The Akt/GSK-3beta axis as a new signaling pathway of the histamine H(3) receptor. *J. Neurochem.* **2007**, *103*, 248–258. [CrossRef] [PubMed]
23. Nordemann, U.; Wifling, D.; Schnell, D.; Bernhardt, G.; Stark, H.; Seifert, R.; Buschauer, A. Luciferase reporter gene assay on human, murine and rat histamine H4 receptor orthologs: Correlations and discrepancies between distal and proximal readouts. *PLoS ONE* **2013**, *8*, e73961. [CrossRef]
24. Kenakin, T. Biased Receptor Signaling in Drug Discovery. *Pharm. Rev.* **2019**, *71*, 267–315. [CrossRef]
25. Kenakin, T. A holistic view of GPCR signaling. *Nat. Biotechnol.* **2010**, *28*, 928–929. [CrossRef]
26. Scott, C.W.; Peters, M.F. Label-free whole-cell assays: Expanding the scope of GPCR screening. *Drug Discov. Today* **2010**, *15*, 704–716. [CrossRef]
27. Aristotelous, T.; Hopkins, A.L.; Navratilova, I. Chapter Twenty-Three—Surface Plasmon Resonance Analysis of Seven-Transmembrane Receptors. In *Methods in Enzymology*; Shukla, A.K., Ed.; Academic Press: Cambridge, MA, USA, 2015; Volume 556, pp. 499–525.
28. Fang, Y. Label-free drug discovery. *Front. Pharm.* **2014**, *5*, 52. [CrossRef]
29. Fang, Y. Non-invasive Optical Biosensor for Probing Cell Signaling. *Sensors* **2007**, *7*, 2316–2329. [CrossRef] [PubMed]
30. Fang, Y.; Ferrie, A.; Fontaine, N.; Ki Yuen, P. Optical biosensors for monitoring dynamic mass redistribution in living cells mediated by epidermal growth factor receptor activation. *Conf. Proc. IEEE Eng. Med. Biol. Soc.* **2005**, *2006*, 666–669. [CrossRef] [PubMed]
31. Carter, R.L.; Grisanti, L.A.; Yu, J.E.; Repas, A.A.; Woodall, M.; Ibetti, J.; Koch, W.J.; Jacobson, M.A.; Tilley, D.G. Dynamic mass redistribution analysis of endogenous beta-adrenergic receptor signaling in neonatal rat cardiac fibroblasts. *Pharmacol. Res. Perspect.* **2014**, *2*, e00024. [CrossRef] [PubMed]
32. Jørgensen, C.V.; Zhou, H.; Seibel, M.J.; Bräuner-Osborne, H. Label-free dynamic mass redistribution analysis of endogenous adrenergic receptor signaling in primary preadipocytes and differentiated adipocytes. *J. Pharmacol. Toxicol. Methods* **2019**, *97*, 59–66. [CrossRef] [PubMed]
33. Ferrie, A.M.; Sun, H.; Zaytseva, N.; Fang, Y. Divergent label-free cell phenotypic pharmacology of ligands at the overexpressed beta(2)-adrenergic receptors. *Sci. Rep.* **2014**, *4*, 3828. [CrossRef] [PubMed]
34. Rocheville, M.; Jerman, J.C. 7TM pharmacology measured by label-free: A holistic approach to cell signalling. *Curr. Opin. Pharm.* **2009**, *9*, 643–649. [CrossRef] [PubMed]
35. Fang, Y.; Li, G.; Ferrie, A.M. Non-invasive optical biosensor for assaying endogenous G protein-coupled receptors in adherent cells. *J. Pharmacol. Toxicol. Methods* **2007**, *55*, 314–322. [CrossRef] [PubMed]
36. Ferrie, A.M.; Wang, C.; Deng, H.; Fang, Y. A label-free optical biosensor with microfluidics identifies an intracellular signalling wave mediated through the beta(2)-adrenergic receptor. *Integr. Biol.* **2013**, *5*, 1253–1261. [CrossRef]
37. Schröder, R.; Janssen, N.; Schmidt, J.; Kebig, A.; Merten, N.; Hennen, S.; Muller, A.; Blattermann, S.; Mohr-Andra, M.; Zahn, S.; et al. Deconvolution of complex G protein-coupled receptor signaling in live cells using dynamic mass redistribution measurements. *Nat. Biotechnol.* **2010**, *28*, 943–949. [CrossRef]
38. Schröder, R.; Schmidt, J.; Blattermann, S.; Peters, L.; Janssen, N.; Grundmann, M.; Seemann, W.; Kaufel, D.; Merten, N.; Drewke, C.; et al. Applying label-free dynamic mass redistribution technology to frame signaling of G protein-coupled receptors noninvasively in living cells. *Nat. Protoc.* **2011**, *6*, 1748–1760. [CrossRef]
39. Tran, E.; Fang, Y. Label-free optical biosensor for probing integrative role of adenylyl cyclase in G protein-coupled receptor signaling. *J. Recept. Signal. Transduct. Res.* **2009**, *29*, 154–162. [CrossRef]
40. West, R.E., Jr.; Moss, J.; Vaughan, M.; Liu, T.; Liu, T.Y. Pertussis toxin-catalyzed ADP-ribosylation of transducin. Cysteine 347 is the ADP-ribose acceptor site. *J. Biol. Chem* **1985**, *260*, 14428–14430. [CrossRef]
41. Grundmann, M.; Merten, N.; Malfacini, D.; Inoue, A.; Preis, P.; Simon, K.; Ruttiger, N.; Ziegler, N.; Benkel, T.; Schmitt, N.K.; et al. Lack of beta-arrestin signaling in the absence of active G proteins. *Nat. Commun.* **2018**, *9*, 341. [CrossRef]
42. Shi, Y.; Sheng, R.; Zhong, T.; Xu, Y.; Chen, X.; Yang, D.; Sun, Y.; Yang, F.; Hu, Y.; Zhou, N. Identification and characterization of ZEL-H16 as a novel agonist of the histamine H3 receptor. *PLoS ONE* **2012**, *7*, e42185. [CrossRef] [PubMed]
43. Gill, D.M.; Meren, R. ADP-ribosylation of membrane proteins catalyzed by cholera toxin: Basis of the activation of adenylate cyclase. *Proc. Natl. Acad. Sci. USA* **1978**, *75*, 3050–3054. [CrossRef] [PubMed]
44. Schrage, R.; Schmitz, A.L.; Gaffal, E.; Annala, S.; Kehraus, S.; Wenzel, D.; Bullesbach, K.M.; Bald, T.; Inoue, A.; Shinjo, Y.; et al. The experimental power of FR900359 to study Gq-regulated biological processes. *Nat. Commun.* **2015**, *6*, 10156. [CrossRef] [PubMed]
45. Lavenus, S.; Simard, E.; Besserer-Offroy, E.; Froehlich, U.; Leduc, R.; Grandbois, M. Label-free cell signaling pathway deconvolution of Angiotensin type 1 receptor reveals time-resolved G-protein activity and distinct AngII and AngIII\IV responses. *Pharmacol. Res.* **2018**, *136*, 108–120. [CrossRef]
46. Carr, R., 3rd; Koziol-White, C.; Zhang, J.; Lam, H.; An, S.S.; Tall, G.G.; Panettieri, R.A., Jr.; Benovic, J.L. Interdicting Gq Activation in Airway Disease by Receptor-Dependent and Receptor-Independent Mechanisms. *Mol. Pharm.* **2016**, *89*, 94–104. [CrossRef]
47. Ruzza, C.; Ferrari, F.; Guerrini, R.; Marzola, E.; Preti, D.; Reinscheid, R.K.; Calo, G. Pharmacological profile of the neuropeptide S receptor: Dynamic mass redistribution studies. *Pharmacol. Res. Perspect.* **2018**, *6*, e00445. [CrossRef]

48. Antony, J.; Kellershohn, K.; Mohr-Andra, M.; Kebig, A.; Prilla, S.; Muth, M.; Heller, E.; Disingrini, T.; Dallanoce, C.; Bertoni, S.; et al. Dualsteric GPCR targeting: A novel route to binding and signaling pathway selectivity. *FASEB J. Off. Publ. Fed. Am. Soc. Exp. Biol.* **2009**, *23*, 442–450. [CrossRef] [PubMed]
49. Kebig, A.; Kostenis, E.; Mohr, K.; Mohr-Andra, M. An optical dynamic mass redistribution assay reveals biased signaling of dualsteric GPCR activators. *J. Recept. Signal. Transduct. Res.* **2009**, *29*, 140–145. [CrossRef] [PubMed]
50. Deng, H.; Wang, C.; Su, M.; Fang, Y. Probing biochemical mechanisms of action of muscarinic M3 receptor antagonists with label-free whole cell assays. *Anal. Chem* **2012**, *84*, 8232–8239. [CrossRef]
51. Watson, S.J.; Brown, A.J.; Holliday, N.D. Differential signaling by splice variants of the human free fatty acid receptor GPR120. *Mol. Pharm.* **2012**, *81*, 631–642. [CrossRef] [PubMed]
52. Qu, L.; Wang, J.; Hou, T.; Zhou, H.; Wang, Z.; Zhang, X.; Liang, X. Systematic characterization of AT1 receptor antagonists with label-free dynamic mass redistribution assays. *J. Pharmacol. Toxicol. Methods* **2020**, *102*, 106682. [CrossRef] [PubMed]
53. Hou, T.; Shi, L.; Wang, J.; Wei, L.; Qu, L.; Zhang, X.; Liang, X. Label-free cell phenotypic profiling and pathway deconvolution of neurotensin receptor-1. *Pharmacol. Res.* **2016**, *108*, 39–45. [CrossRef] [PubMed]
54. Milligan, G.; Inoue, A. Genome Editing Provides New Insights into Receptor-Controlled Signalling Pathways. *Trends Pharmacol. Sci.* **2018**, *39*, 481–493. [CrossRef] [PubMed]
55. Lukasheva, V.; Devost, D.; Le Gouill, C.; Namkung, Y.; Martin, R.D.; Longpré, J.-M.; Amraei, M.; Shinjo, Y.; Hogue, M.; Lagacé, M.; et al. Signal profiling of the β1AR reveals coupling to novel signalling pathways and distinct phenotypic responses mediated by β1AR and β2AR. *Sci. Rep.* **2020**, *10*, 8779. [CrossRef]
56. Young, J.M.; Timmerman, H.; Thurmond, R.; Stark, H.; Shankley, N.P.; Seifert, R.; Schwartz, J.-C.; Schunack, W.; Panula, P.; Liu, S.; et al. Histamine receptors (version 2019.4) in the IUPHAR/BPS Guide to Pharmacology Database. *IUPHAR/BPS Guide Pharmacol. CITE* **2019**, *2019*. [CrossRef]
57. Panula, P.; Chazot, P.L.; Cowart, M.; Gutzmer, R.; Leurs, R.; Liu, W.L.; Stark, H.; Thurmond, R.L.; Haas, H.L. International Union of Basic and Clinical Pharmacology. XCVIII. Histamine Receptors. *Pharm. Rev.* **2015**, *67*, 601–655. [CrossRef]
58. Tiligada, E.; Ennis, M. Histamine pharmacology: From Sir Henry Dale to the 21st century. *Br. J. Pharm.* **2018**, *177*, 469–489. [CrossRef] [PubMed]
59. Okashah, N.; Wan, Q.; Ghosh, S.; Sandhu, M.; Inoue, A.; Vaidehi, N.; Lambert, N.A. Variable G protein determinants of GPCR coupling selectivity. *Proc. Natl. Acad. Sci. USA* **2019**, *116*, 12054–12059. [CrossRef]
60. Avet, C.; Mancini, A.; Breton, B.; Le Gouill, C.; Hauser, A.S.; Normand, C.; Kobayashi, H.; Gross, F.; Hogue, M.; Lukasheva, V.; et al. Selectivity Landscape of 100 Therapeutically Relevant GPCR Profiled by an Effector Translocation-Based BRET Platform. *bioRxiv* **2020**. [CrossRef]
61. Esbenshade, T.A.; Kang, C.H.; Krueger, K.M.; Miller, T.R.; Witte, D.G.; Roch, J.M.; Masters, J.N.; Hancock, A.A. Differential activation of dual signaling responses by human H1 and H2 histamine receptors. *J. Recept. Signal. Transduct. Res.* **2003**, *23*, 17–31. [CrossRef]
62. Atwood, B.K.; Lopez, J.; Wager-Miller, J.; Mackie, K.; Straiker, A. Expression of G protein-coupled receptors and related proteins in HEK293, AtT20, BV2, and N18 cell lines as revealed by microarray analysis. *BMC Genom.* **2011**, *12*, 14. [CrossRef]
63. Stallaert, W.; van der Westhuizen, E.T.; Schonegge, A.M.; Plouffe, B.; Hogue, M.; Lukashova, V.; Inoue, A.; Ishida, S.; Aoki, J.; Le Gouill, C.; et al. Purinergic Receptor Transactivation by the beta2-Adrenergic Receptor Increases Intracellular Ca(2+) in Nonexcitable Cells. *Mol. Pharm.* **2017**, *91*, 533–544. [CrossRef] [PubMed]
64. Devost, D.; Sleno, R.; Petrin, D.; Zhang, A.; Shinjo, Y.; Okde, R.; Aoki, J.; Inoue, A.; Hebert, T.E. Conformational Profiling of the AT1 Angiotensin II Receptor Reflects Biased Agonism, G Protein Coupling, and Cellular Context. *J. Biol. Chem.* **2017**, *292*, 5443–5456. [CrossRef] [PubMed]
65. Bruysters, M.; Pertz, H.H.; Teunissen, A.; Bakker, R.A.; Gillard, M.; Chatelain, P.; Schunack, W.; Timmerman, H.; Leurs, R. Mutational analysis of the histamine H1-receptor binding pocket of histaprodifens. *Eur. J. Pharm.* **2004**, *487*, 55–63. [CrossRef] [PubMed]
66. Pertz, H.H.; Gornemann, T.; Schurad, B.; Seifert, R.; Strasser, A. Striking differences of action of lisuride stereoisomers at histamine H_1 receptors. *Naunyn-Schmiedeberg's Arch. Pharmacol.* **2006**, *374*, 215–222. [CrossRef]
67. Moguilevsky, N.; Varsalona, F.; Noyer, M.; Gillard, M.; Guillaume, J.P.; Garcia, L.; Szpirer, C.; Szpirer, J.; Bollen, A. Stable expression of human H1-histamine-receptor cDNA in Chinese hamster ovary cells. Pharmacological characterisation of the protein, tissue distribution of messenger RNA and chromosomal localisation of the gene. *Eur. J. Biochem* **1994**, *224*, 489–495. [CrossRef]
68. Sibley, D.R.; Mahan, L.C.; Creese, I. Dopamine receptor binding on intact cells. Absence of a high-affinity agonist-receptor binding state. *Mol. Pharm.* **1983**, *23*, 295–302.
69. Baumeister, P.; Erdmann, D.; Biselli, S.; Kagermeier, N.; Elz, S.; Bernhardt, G.; Buschauer, A. [(3)H]UR-DE257: Development of a tritium-labeled squaramide-type selective histamine H2 receptor antagonist. *ChemMedChem* **2015**, *10*, 83–93. [CrossRef] [PubMed]
70. Igel, P.; Schnell, D.; Bernhardt, G.; Seifert, R.; Buschauer, A. Tritium-labeled N(1)-[3-(1H-imidazol-4-yl)propyl]-N(2)-propionylguanidine ([(3)H]UR-PI294), a high-affinity histamine H(3) and H(4) receptor radioligand. *ChemMedChem* **2009**, *4*, 225–231. [CrossRef] [PubMed]

71. Bosma, R.; Witt, G.; Vaas, L.A.I.; Josimovic, I.; Gribbon, P.; Vischer, H.F.; Gul, S.; Leurs, R. The Target Residence Time of Antihistamines Determines Their Antagonism of the G Protein-Coupled Histamine H1 Receptor. *Front. Pharm.* **2017**, *8*, 667. [CrossRef]
72. Tran, E.; Ye, F. Duplexed label-free G protein–coupled receptor assays for high-throughput screening. *J. Biomol Screen* **2008**, *13*, 975–985. [CrossRef] [PubMed]
73. Lieb, S.; Michaelis, S.; Plank, N.; Bernhardt, G.; Buschauer, A.; Wegener, J. Label-free analysis of GPCR-stimulation: The critical impact of cell adhesion. *Pharmacol. Res.* **2016**, *108*, 65–74. [CrossRef]
74. Tran, E.; Sun, H.; Fang, Y. Dynamic mass redistribution assays decode surface influence on signaling of endogenous purinergic P2Y receptors. *Assay Drug Dev. Technol.* **2012**, *10*, 37–45. [CrossRef] [PubMed]
75. Malfacini, D.; Simon, K.; Trapella, C.; Guerrini, R.; Zaveri, N.T.; Kostenis, E.; Calo, G. NOP receptor pharmacological profile-A dynamic mass redistribution study. *PLoS ONE* **2018**, *13*, e0203021. [CrossRef]
76. Wifling, D.; Loffel, K.; Nordemann, U.; Strasser, A.; Bernhardt, G.; Dove, S.; Seifert, R.; Buschauer, A. Molecular determinants for the high constitutive activity of the human histamine H4 receptor: Functional studies on orthologues and mutants. *Br. J. Pharm.* **2015**, *172*, 785–798. [CrossRef] [PubMed]
77. Bakker, R.A.; Wieland, K.; Timmerman, H.; Leurs, R. Constitutive activity of the histamine H1 receptor reveals inverse agonism of histamine H1 receptor antagonists. *Eur. J. Pharmacol.* **2000**, *387*, R5–R7. [CrossRef]
78. Wieland, K.; Bongers, G.; Yamamoto, Y.; Hashimoto, T.; Yamatodani, A.; Menge, W.M.; Timmerman, H.; Lovenberg, T.W.; Leurs, R. Constitutive activity of histamine h(3) receptors stably expressed in SK-N-MC cells: Display of agonism and inverse agonism by H(3) antagonists. *J. Pharmacol. Exp. Ther.* **2001**, *299*, 908–914.
79. Schihada, H.; Ma, X.; Zabel, U.; Vischer, H.F.; Schulte, G.; Leurs, R.; Pockes, S.; Lohse, M.J. Development of a Conformational Histamine H3 Receptor Biosensor for the Synchronous Screening of Agonists and Inverse Agonists. *ACS Sens.* **2020**, *5*, 1734–1742. [CrossRef]
80. Horing, C.; Seibel, U.; Tropmann, K.; Gratz, L.; Monnich, D.; Pitzl, S.; Bernhardt, G.; Pockes, S.; Strasser, A. A Dynamic, Split-Luciferase-Based Mini-G Protein Sensor to Functionally Characterize Ligands at All Four Histamine Receptor Subtypes. *Int. J. Mol. Sci.* **2020**, *21*, 8440. [CrossRef]
81. Preuss, H.; Ghorai, P.; Kraus, A.; Dove, S.; Buschauer, A.; Seifert, R. Constitutive activity and ligand selectivity of human, guinea pig, rat, and canine histamine H2 receptors. *J. Pharmacol. Exp. Ther.* **2007**, *321*, 983–995. [CrossRef]
82. Seifert, R.; Wenzel-Seifert, K. Constitutive activity of G-protein-coupled receptors: Cause of disease and common property of wild-type receptors. *Naunyn-Schmiedeberg's Arch. Pharmacol.* **2002**, *366*, 381–416. [CrossRef]
83. Kenakin, T. Efficacy as a Vector: The Relative Prevalence and Paucity of Inverse Agonism. *Mol. Pharmacol.* **2004**, *65*, 2–11. [CrossRef] [PubMed]
84. Scheff, J.D.; Almon, R.R.; Dubois, D.C.; Jusko, W.J.; Androulakis, I.P. Assessment of pharmacologic area under the curve when baselines are variable. *Pharm Res.* **2011**, *28*, 1081–1089. [CrossRef] [PubMed]
85. Elmer, P. *Development Guide for. Cell-Based Label.-Free Assays*, 1st ed.; Perkin Elmer: Waltham, MA, USA, 2013.
86. Deng, H.; Sun, H.; Fang, Y. Label-free cell phenotypic assessment of the biased agonism and efficacy of agonists at the endogenous muscarinic M3 receptors. *J. Pharmacol. Toxicol. Methods* **2013**, *68*, 323–333. [CrossRef] [PubMed]
87. Fang, Y. The development of label-free cellular assays for drug discovery. *Expert Opin. Drug Discov.* **2011**, *6*, 1285–1298. [CrossRef] [PubMed]
88. Chio, C.L.; Lajiness, M.E.; Huff, R.M. Activation of heterologously expressed D3 dopamine receptors: Comparison with D2 dopamine receptors. *Mol. Pharm.* **1994**, *45*, 51–60.
89. Bartole, E.; Grätz, L.; Littmann, T.; Wifling, D.; Seibel, U.; Buschauer, A.; Bernhardt, G. UR-DEBa242: A Py-5-Labeled Fluorescent Multipurpose Probe for Investigations on the Histamine H3 and H4 Receptors. *J. Med. Chem.* **2020**, *63*, 5297–5311. [CrossRef] [PubMed]
90. Khoury, E.; Clément, S.; Laporte, S.A. Allosteric and Biased G Protein-Coupled Receptor Signaling Regulation: Potentials for New Therapeutics. *Front. Endocrinol.* **2014**, *5*, 38. [CrossRef]
91. Inoue, A.; Raimondi, F.; Kadji, F.M.N.; Singh, G.; Kishi, T.; Uwamizu, A.; Ono, Y.; Shinjo, Y.; Ishida, S.; Arang, N.; et al. Illuminating G-Protein-Coupling Selectivity of GPCRs. *Cell* **2019**, *177*, 1933–1947.e25. [CrossRef]
92. Lehmann, D.M.; Seneviratne, A.M.; Smrcka, A.V. Small molecule disruption of G protein beta gamma subunit signaling inhibits neutrophil chemotaxis and inflammation. *Mol. Pharm.* **2008**, *73*, 410–418. [CrossRef] [PubMed]
93. Kim, Y.S.; Kim, Y.B.; Kim, W.B.; Lee, S.W.; Oh, S.B.; Han, H.C.; Lee, C.J.; Colwell, C.S.; Kim, Y.I. Histamine 1 receptor-Gbetagamma-cAMP/PKA-CFTR pathway mediates the histamine-induced resetting of the suprachiasmatic circadian clock. *Mol. Brain* **2016**, *9*, 49. [CrossRef] [PubMed]
94. Bonacci, T.M.; Mathews, J.L.; Yuan, C.; Lehmann, D.M.; Malik, S.; Wu, D.; Font, J.L.; Bidlack, J.M.; Smrcka, A.V. Differential targeting of Gbetagamma-subunit signaling with small molecules. *Science* **2006**, *312*, 443–446. [CrossRef] [PubMed]
95. Houston, C.; Wenzel-Seifert, K.; Burckstummer, T.; Seifert, R. The human histamine H2-receptor couples more efficiently to Sf9 insect cell Gs-proteins than to insect cell Gq-proteins: Limitations of Sf9 cells for the analysis of receptor/Gq-protein coupling. *J. Neurochem.* **2002**, *80*, 678–696. [CrossRef]
96. Oda, T.; Morikawa, N.; Saito, Y.; Masuho, Y.; Matsumoto, S. Molecular cloning and characterization of a novel type of histamine receptor preferentially expressed in leukocytes. *J. Biol. Chem.* **2000**, *275*, 36781–36786. [CrossRef]

97. Plank, N. Dimeric Histamine H2 Receptor Agonists as Molecular Tools and Genetically Engineered HEK293T Cells as an Assay Platform to Unravel Signaling Pathways of hH1R and hH2R. Ph.D. Thesis, University of Regensburg, Regensburg, Germany, 2015. [CrossRef]
98. Bakker, R.A.; Nicholas, M.W.; Smith, T.T.; Burstein, E.S.; Hacksell, U.; Timmerman, H.; Leurs, R.; Brann, M.R.; Weiner, D.M. In vitro pharmacology of clinically used central nervous system-active drugs as inverse H-1 receptor agonists. *J. Pharmacol. Exp. Ther.* **2007**, *322*, 172–179. [CrossRef] [PubMed]
99. Casale, T.B.; Rodbard, D.; Kaliner, M. Characterization of histamine H-1 receptors on human peripheral lung. *Biochem. Pharmacol.* **1985**, *34*, 3285–3292. [CrossRef]
100. Fitzsimons, C.P.; Monczor, F.; Fernandez, N.; Shayo, C.; Davio, C. Mepyramine, a histamine H1 receptor inverse agonist, binds preferentially to a G protein-coupled form of the receptor and sequesters G protein. *J. Biol. Chem.* **2004**, *279*, 34431–34439. [CrossRef]
101. Höring, C.; Conrad, M.; Söldner, C.A.; Wang, J.; Sticht, H.; Strasser, A.; Miao, Y. Specific Engineered G Protein Coupling to Histamine Receptors Revealed from Cellular Assay Experiments and Accelerated Molecular Dynamics Simulations. *Int. J. Mol. Sci.* **2021**, *22*, 10047.
102. Bosma, R.; Moritani, R.; Leurs, R.; Vischer, H.F. BRET-based beta-arrestin2 recruitment to the histamine H1 receptor for investigating antihistamine binding kinetics. *Pharmacol. Res.* **2016**, *111*, 679–687. [CrossRef]
103. Fernandez, N.; Monczor, F.; Baldi, A.; Davio, C.; Shayo, C. Histamine H2 receptor trafficking: Role of arrestin, dynamin, and clathrin in histamine H2 receptor internalization. *Mol. Pharm.* **2008**, *74*, 1109–1118. [CrossRef]
104. Nijmeijer, S.; Vischer, H.F.; Rosethorne, E.M.; Charlton, S.J.; Leurs, R. Analysis of multiple histamine H(4) receptor compound classes uncovers Galphai protein- and beta-arrestin2-biased ligands. *Mol. Pharm.* **2012**, *82*, 1174–1182. [CrossRef] [PubMed]
105. Micallef, S.; Stark, H.; Sasse, A. Polymorphisms and genetic linkage of histamine receptors. *Life Sci.* **2013**, *93*, 487–494. [CrossRef] [PubMed]
106. Leary, P.J.; Kronmal, R.A.; Bluemke, D.A.; Buttrick, P.M.; Jones, K.L.; Kao, D.P.; Kawut, S.M.; Krieger, E.V.; Lima, J.A.; Minobe, W.; et al. Histamine H2 Receptor Polymorphisms, Myocardial Transcripts, and Heart Failure (from the Multi-Ethnic Study of Atherosclerosis and Beta-Blocker Effect on Remodeling and Gene Expression Trial). *Am. J. Cardiol.* **2018**, *121*, 256–261. [CrossRef] [PubMed]
107. Gu, J.; Mao, X.H.; Yang, X.Z.; Ao, H.F.; Zhang, Z.; Li, Y. Histamine H4 receptor gene polymorphisms: A potential predictor of oral H1 antihistamine efficacy for allergic rhinitis. *Int. Forum. Allergy Rhinol.* **2017**, *7*, 268–275. [CrossRef] [PubMed]
108. Chu, J.T. Histamine H1 receptor gene polymorphism acts as a biological indicator of the prediction of therapeutic efficacy in patients with allergic rhinitis in the Chinese Han population. *J. Cell Biochem.* **2019**, *120*, 164–170. [CrossRef]
109. Wei, Z.; Wang, L.; Zhang, M.; Xuan, J.; Wang, Y.; Liu, B.; Shao, L.; Li, J.; Zeng, Z.; Li, T.; et al. A pharmacogenetic study of risperidone on histamine H3 receptor gene (HRH3) in Chinese Han schizophrenia patients. *J. Psychopharmacol.* **2012**, *26*, 813–818. [CrossRef]
110. Li, J.; Chen, W.; Peng, C.; Zhu, W.; Liu, Z.; Zhang, W.; Su, J.; Li, J.; Chen, X. Human H1 receptor (HRH1) gene polymorphism is associated with the severity of side effects after desloratadine treatment in Chinese patients with chronic spontaneous uticaria. *Pharm. J.* **2020**, *20*, 87–93. [CrossRef] [PubMed]
111. Rosier, N.; Gratz, L.; Schihada, H.; Moller, J.; Isbilir, A.; Humphrys, L.J.; Nagl, M.; Seibel, U.; Lohse, M.J.; Pockes, S. A Versatile Sub-Nanomolar Fluorescent Ligand Enables NanoBRET Binding Studies and Single-Molecule Microscopy at the Histamine H3 Receptor. *J. Med. Chem.* **2021**, *64*, 11695–11708. [CrossRef] [PubMed]
112. Kagermeier, N.; Werner, K.; Keller, M.; Baumeister, P.; Bernhardt, G.; Seifert, R.; Buschauer, A. Dimeric carbamoylguanidine-type histamine H2 receptor ligands: A new class of potent and selective agonists. *Bioorg. Med. Chem.* **2015**, *23*, 3957–3969. [CrossRef]
113. Yung-Chi, C.; Prusoff, W.H. Relationship between the inhibition constant (KI) and the concentration of inhibitor which causes 50 per cent inhibition (I50) of an enzymatic reaction. *Biochem. Pharmacol.* **1973**, *22*, 3099–3108. [CrossRef]